

Contents lists available at ScienceDirect

Tectonophysics

journal homepage: www.elsevier.com/locate/tecto





Geometry and kinematics of the western part of the NE Qaidam Basin: Implications for the growth of the Tibetan Plateau

Liang Luo ^{a,b,*}, John W. Geissman ^{c,d}, Xu Zeng ^{a,b}, Bo Wang ^e, Fei Zhou ^e, Yi Zhang ^e, Shaohang Yang ^{a,b}, Yangfan Zhou ^{a,b}

- ^a State Key Laboratory of Petroleum Resources and Prospecting, China University of Petroleum (Beijing), Beijing 102249, China
- ^b College of Geosciences, China University of Petroleum (Beijing), Beijing 102249, China
- ^c Department of Geosciences, The University of Texas at Dallas, Richardson, TX 75080-3021, USA
- ^d Department of Earth and Planetary Sciences, University of New Mexico, Albuquerque, NM 87131-0001, USA
- e Qinghai Oilfield Company, PetroChina, Dunhuang 736200, China

ARTICLE INFO

Keywords: NE Qaidam Basin Tibetan Plateau Altyn Tagh Fault Qilian Shan Dextral

ABSTRACT

Based on field geology, seismic reflection profiling data and isopach maps, the structural deformation pattern, timing of deformation, and mechanism of formation of the western part of the NE Qaidam Basin (including the Pingtai Uplift, Lenghu and Eboliang structural belts) during the Mesozoic and Cenozoic eras have been investigated. Several anticlines in the Lenghu and Eboliang structural belts are generally characterized by double fault systems at different structural levels. At shallower crustal levels, a thrust fault system dominates and at lower levels positive flower structures accommodate oblique shortening, and these are mainly separated by weak strata layers in the Upper Xiaganchaigou Formation, of late Eocene age. Left-step en echelon distributed normal faults and trailing extensional imbricate fan structures consistently demonstrate that the Lenghu and Eboliang structural belts are dominated by dextral transpressional deformation. The western part of the NE Qaidam Basin experienced an initial stage of extension in the Jurassic, which was associated with the formation of several NWstriking normal faults. We hypothesize that most of the deep compressional structures and shallow anticlines were formed due to the SW-directed thrusting of the Qilian Shan since the early Eocene, as a far-field effect of the Indo-Asian "hard" collision. The NNE-directed shortening was associated with dextral transpressional deformation within the western part of the NE Qaidam Basin that took place after the deposition of the Shangyoushashan Formation, of middle-late Miocene age. We interpret this phase of deformation to have been an integral part of the pulsed growth of the whole Tibetan Plateau.

1. Introduction

Continued Indo-Asian collision since circa 60–45 Ma has driven the growth and crustal deformation of the Tibetan Plateau (Garzanti and Van Haver, 1988; Rowley, 1996; Green et al., 2008; Dupont-Nivet et al., 2010; Najman et al., 2010; Hu et al., 2015, 2016; Huang et al., 2015). The history of development of the Tibetan Plateau and associated processes has been a highly debatable topic in international geologic research (Royden et al., 1997; Tapponnier et al., 2001; Molnar and Stock, 2009; Clark et al., 2010; Zhuang et al., 2011; Clark, 2012; Bush et al., 2016; Cheng et al., 2018). The Qaidam basin, situated in the northern Tibetan Plateau (Fig. 1a), is filled with over 13 km of Cenozoic detrital sedimentary rocks in its depositional center around Yiliping.

This sequence preserves a complete record of the intraplate response to the Indo-Asian collision and thus is an ideal place for exploring the growth of Tibetan Plateau (Molnar and Tapponnier, 1975; Wittlinger et al., 1998; Yue and Liou, 1999; Jolivet et al., 2001; Yin et al., 2002; Yue et al., 2004a, 2004b; Searle et al., 2011; Cheng et al., 2015a, 2016; Zhang et al., 2018).

Foredeep deposits accumulated along the rims of the typical foreland basins in western China, such as the Sichuan Basin (Hubbard and Shaw, 2009; Jia et al., 2006). In the center of many of these basins, there is no obvious evidence of strong deformation. However, the interior of the Qaidam Basin is dominated by faulting and folding (Yin et al., 2008b) and these structures can be clearly observed in the field and any form of remote sensing approaches. No foreland depressions are formed along

^{*} Corresponding author at: State Key Laboratory of Petroleum Resources and Prospecting, China University of Petroleum (Beijing), Beijing 102249, China. E-mail address: luoliang1225@163.com (L. Luo).

the margins (Zhou et al., 2006; Yin et al., 2008b; Cheng et al., 2014, 2015a). Extensive efforts have been devoted to address the Cenozoic deformation history and evolution of the Qaidam Basin, and most of them have been concentrated in the northwest part of Qaidam Basin (Cheng et al., 2015b, 2017, 2018, Mao et al., 2016; Zhang et al., 2018;

Bian et al., 2019; Du et al., 2019; Liu et al., 2019; Zhang et al., 2020). At the same time, the western part of the NE Qaidam Basin has received very limited attention to date.

Here, we present new seismic data and associated interpretation, surface geology information and isopach map analysis to investigate the

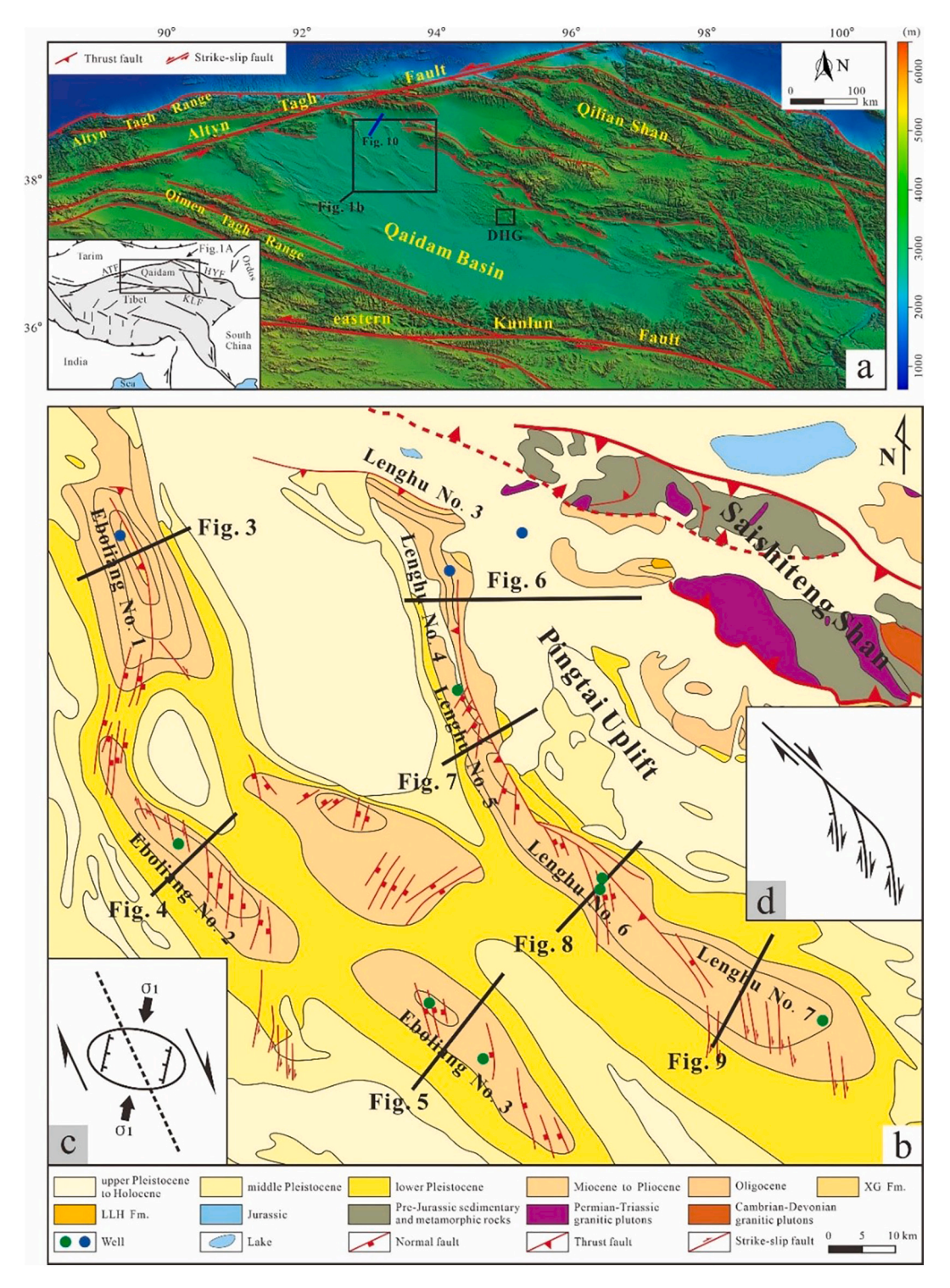


Fig. 1. (a) Location map with major tectonic elements of the northern Tibetan Plateau (modified from Liu et al., 2019). The DEM (digital elevation model) shows the topography of the Qaidam Basin and surrounding mountains. Short blue solid line represents location of seismic profile in Fig. 10. (b) Simplified geologic map of the western part of the NE Qaidam Basin and its surrounding areas, adapted from Geological Map of the Qaidam Basin. Blue dots represent the locations of the wells drilled into the Lulehe Formation, while green dots represent the locations of the wells drilled into the younger strata. Short black solid lines represent locations of seismic profiles in Fig. 3–9, respectively. The normal (c) and strike-slip (d) faults with limited displacement can be explained by the principal strike-slip fault zone, which are modified after Sylvester (1988) and Woodcock and Fischer (1986). (For interpretation of the references to colour in this figure legend, the reader is referred to the web version of this article.)

geometry and kinematics of the western part of the NE Qaidam Basin, which lies at the juncture of the two most important boundaries of the Qaidam Basin, the Altyn Tagh Fault (ATF) and the Qilian Shan (Fig. 1a). The results of this study further elucidate the history of the Indo-Asian collision and the subsequent Tibetan Plateau growth by demonstrating their effects on the western part of the NE Qaidam Basin and the ATF.

2. Geologic setting

2.1. Qilian Shan

The NW-SE trending Qilian Shan, with an average elevation of 4 km, marks the northern boundary of the Qaidam basin and the northeast edge of the Tibetan Plateau (Fig. 1a). Its formation has been attributed to the development of early-middle Paleozoic orogenic suture belts, which are composed of numerous thrust slices of deformed lower Paleozoic metasedimentary and metavolcanic strata (Yin and Harrison, 2000; Xiao et al., 2009). Different parts of the Qilian Shan fold-thrust belt are thought to have been sutured to the Qaidam block during the middle Paleozoic at different intervals (Yin and Harrison, 2000). The modern Qilian Shan, exposing folds, thrusts, and strike-slip faults that accommodate considerable horizontal shortening and lateral motion of the crust, was reactivated and formed following the initiation of the Indo-Asian collision (Yin and Harrison, 2000; Clark, 2012). Currently, the timing of Cenozoic deformation of the Qilian Shan is vigorously debated. Several lines of evidence suggest an onset of contractional deformation shortly after the initiation of the Indo-Asian collision (Yin et al., 2002, 2008a, 2008b; Dupont-Nivet et al., 2004; Dayem et al., 2009; Clark et al., 2010; Duvall et al., 2011), and recent studies indicate that the Qilian Shan underwent a renewed episode of topographic growth during the late Miocene (Fang et al., 2005; Bovet et al., 2009; Zheng et al., 2010; Zhuang et al., 2011). Alternatively, some workers consider the late Miocene to Quaternary phase of deformation as the key component of crustal shortening in the area (Tapponnier et al., 1990; Tapponnier et al., 2001; Meyer et al., 1998).

2.2. Altyn Tagh Fault

The over 1600 km long left-lateral strike-slip ATF, with an ENE-WSW strike, defines the northwest boundary of the Qaidam basin, and links the western Kunlun Shan to the southwest and the Qilian Shan to the northeast (Fig. 1a). This left-lateral fault system has experienced a multistage tectonic history, from Mesozoic-early Paleogene time to the present (Tapponnier et al., 1986; Jolivet et al., 1999, 2001, 2003; Yue and Liou, 1999; Ritts and Biffi, 2000; Chen et al., 2001; Delville et al., 2001; Sobel et al., 2001; Yin et al., 2002; Wang et al., 2005, 2006; Wu et al., 2012; Cheng et al., 2015a; Wu et al., 2019; Yun et al., 2020). The timing of inception of Cenozoic left-lateral strike-slip movement on the ATF is still debated, with estimates ranging from early Eocene (Yin et al., 2002) to late Eocene-early Oligocene as supported by thermochronologic data (Chen et al., 2001) and sedimentology (Meng et al., 2001; Yue et al., 2001; Ritts et al., 2004), and, lastly, to middle Miocene time based on structural analysis, sedimentology and apatite fission track data (Burchfiel et al., 1989; Wang, 1997; Meyer et al., 1998; Wan et al., 2001; Chen et al., 2002; Wang et al., 2010; Wu et al., 2012; Zhang et al., 2018). In addition, estimates of the total magnitude of displacement range from approximately tens of kilometers (Wang, 1997; Chen et al., 2004) to ~400–500 km (Peltzer and Tapponnier, 1988; Yin and Harrison, 2000; Gehrels et al., 2003; Yue et al., 2005) or >1000 km (Chinese State Bureau of Seismology, 1992).

2.3. Western part of the NE Qaidam Basin

The Qaidam Basin is the largest petroliferous basin within the northern Tibetan Plateau (Fu et al., 2015). It is a triangle-shaped basin bounded by the Qilian Shan to the northeast, the ATF to the northwest,

and Qimen Tagh Range and Eastern Kunlun Fault to the south (Fig. 1a). The pattern of Cenozoic tectonic deformation is complicated throughout the entire northern Qaidam Basin due to the remote stress caused by northward expansion and wedging of the Indian plate and drag produced by sinistral strike-slip movement of the ATF (Wang et al., 2006; Li et al., 2017).

The western part of the NE Qaidam Basin consists of three NW-SE trending structural belts: the Pingtai Uplift, the Lenghu Structural Belt and the Eboliang Structural Belt (Fig. 1b). The Pingtai Uplift is situated on the west margin of Saishiteng Shan, which is a part of Qilian Shan. The arcuate Lenghu Structural Belt is composed of five anticlines, named Lenghu No. 3, No. 4, No. 5, No. 6 and No. 7 anticlines (Fig. 1b). The arcuate Eboliang Structural Belt includes three anticlines, named Eboliang No. 1, No. 2 and No. 3 anticlines (Fig. 1b). The western part of the NE Qaidam Basin is widely capped by Quaternary deposits. Strata of Neogene age are mainly exposed in the cores of the anticlines and there are exposures of Paleogene strata in a few areas of the Pingtai Uplift (Fig. 1b).

Upper Jurassic and Cretaceous strata are not exposed at the surface in the western part of the NE Qaidam Basin. Lithologic patterns and fossil assemblages, such as ostracod, pollen, and spores (Huo, 1990) have been used by several workers to subdivide the terrestrial Cenozoic deposits in the Qaidam Basin. The absolute ages of these sequences are well determined based on magnetic polarity stratigraphy (Yang et al., 1992; Ye et al., 1993; Sun et al., 2005; Zhang, 2006; Fang et al., 2007; Gao et al., 2009). The stratigraphic units are listed in Fig. 2. The boundaries between these formations have been labeled by petroleum geologists as the following regional surfaces, and we refer to these repeatedly in this contribution: T6 (approximate age of 201.3 Ma), TR (approximate age of 53.5 Ma), T5 (approximate age of 43.8 Ma), T4 (approximate age of 40.5 Ma), T3 (approximate age of 35.5 Ma), T2 (approximate age of 23.0 Ma), T2' (approximate age of 15.3 Ma), T1 (approximate age of 8.1 Ma), and T0 (approximate age of 2.5 Ma) (Fig. 2) (Fu et al., 2015; Mao et al., 2016; Cheng et al., 2018).

3. Methods

In order to decipher the tectonic pattern and onset of deformation in the different parts of the western part of the NE Qaidam Basin, eight high-quality 3D and 2D seismic reflection profiles acquired by the Qinghai Oilfield Company, PetroChina, have been selected and interpreted. Based on synthetic seismograms of several wells (Fig. 1c), the eight regional surfaces described above (T6, TR, T5, T4, T3, T2, T2' and T1) were calibrated. The interpretation of the regional surfaces was mostly based on extension of cross-well seismic profiles. The seismic data were interpreted using the LandMark software. All the maps were produced using CorelDRAW software (Version X7) (http://www.corel.com/cn/).

4. Surface and subsurface structural interpretation

Our surface structural interpretation is guided by previously unpublished data obtained by the Qinghai Oilfield Corporation, Petro-China, and compiled as the Geological Map of the Qaidam Basin. Critical surface structural features are summarized as follows. First, almost no map-scale fault is expressed on the outcrop map of the Pingtai Uplift (Fig. 1b). Second, four anticlines, including Lenghu No. 5, Lenghu No. 6, Eboliang No. 2 and Eboliang No. 3, are characterized by the presence of several normal faults at shallow structural levels, the traces of which are oriented at an acute angle to the trend of the fold axes of the anticlines (Fig. 1b). Third, the NW-trending tightly folded Lenghu No. 7 Anticline, located in the southernmost part of the Lenghu Structural Belt, is dominated by numerous parallel faults on its crest, most of which are interpreted to be strike-slip faults (Fig. 1b). The magnitudes of the displacements along these strike-slip faults based on surface exposures are relatively limited.

Period	Epoch	Age (Ma)	Formation	Seismic reflector	Symbol	Lithology
Neogene	Holocene	-0.01	Dabuxun-Yanqiao	T2' — T2 — T3 — T4 — T5 —	Q ₂₋₄	gray, grayish yellow conglomerate, pebbled sandstone, grayish, grayish white sandy mudstone
	Pleistocene	-2.58 2. .	Qigequan (QGQ)		Q_1q	
	Pliocene	-5.33	Shizigou (SZG)		N ₂ ³ S	upper part: grayish white, brown mudstone, and interlayed siltstone lower part: pebbled sandstone, siltstone, pelitic siltstone and mudstone
	Miocene		Shangyoushashan (SY)		N ₂ ² sy	gray, dark gray mudstone intercalated with dark gray calcareous mudstone
		15	Xiayoushashan (XY)		N ₂ ¹ xy	upper part: thick gray mudstone intercalated with marlstone and limestone lower part: gray mudstone intercalated with thin marlstone and siltstone
Paleogene	Oligocene	-23.03 23.0 - -33.9 35.5 - 40.5 -	Shangganchaigou (SG)		N ₁ sg	gray mudstone intercalated with siltstone
	Eocene		Upper (UXG)		$E_3^2 xg$	evaporites, grayish mudstone and calcareous mudstone intercalated with politic siltstone
			Lower (LXG)		E ₃ ¹xg	brown mudstone and interlayered fine-grained sandstone
		43.5 53.5	Lulehe (LLH)		E ₁₁₂ 1	upper part: mudstone interlayered with siltstone lower part: mostly conglomerate
	Paleocene	-56.0				
Cretaceous		-66.0				
Jurassic		201.3±0.2		Т6		

Fig. 2. Stratigraphy and lithologic unit descriptions within the western part of the NE Qaidam Basin. The Cenozoic stratigraphy of the basin has been defined and dated in detail using magnetostratigraphy, palynology, and paleontology studies within the entire basin (Yang et al., 1992; Sun et al., 2005; 2007; Song, 2006; Zhang, 2006; Fang et al., 2007; Lu and Xiong, 2009; Zhang et al., 2012, 2014; Ke et al., 2013). E₁₊₂l, Lulehe Formation; E₃¹xg, Lower Xiaganchaigou Formation; E₃²xg, Upper Xiaganchaigou Formation; N₁sg, Shangganchaigou Formation; N₂¹xy, Xiayoushashan Formation; N₂²sy, Shangyoushashan Formation; N₂³s, Shizigou Formation; Q₁q, Qigequan Formation; Q₂₋₄, Dabuxun-Yanqiao Formation.

As noted above, considerable high-resolution seismic data have been collected in conjunction with hydrocarbon exploration efforts in the western part of the NE Qaidam Basin over the past decade. We interpret seven E and NE-trending seismic profiles that are about orthogonal to

the axes of major folds based on surface outcrop information and subsurface core logging data to evaluate structures associated with subsurface deformation (Fig. 1b).

The Eboliang No. 1 Anticline is a nearly symmetric thrust-related

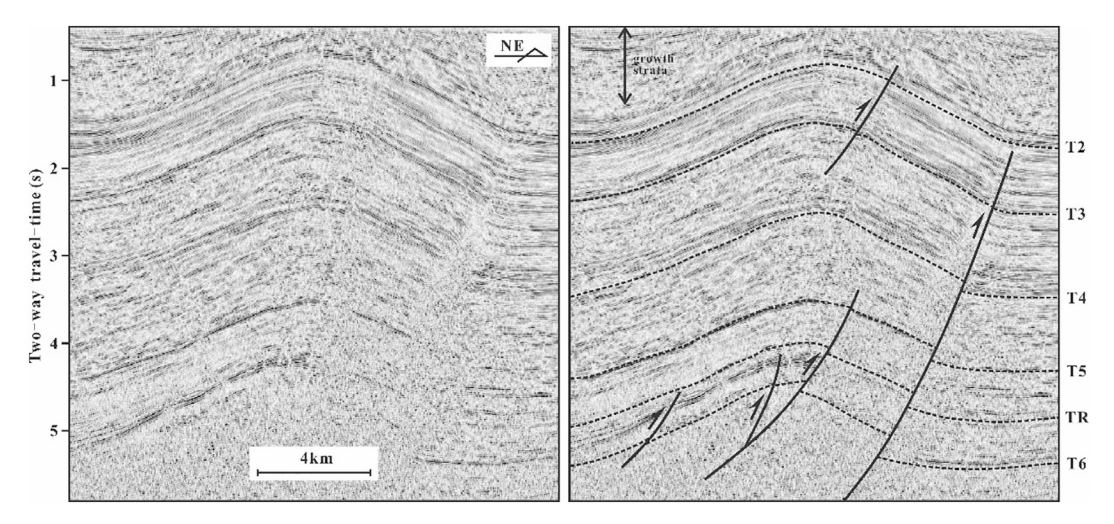


Fig. 3. Seismic cross section across the Eboliang No. 1 Anticline. (left) Original, (right), with structural interpretations. The location of profile is showed in Fig. 1b.

fold, with its blind SW-dipping main thrust fault being rooted at the basement, which we define as the rocks older than Jurassic. With the fault slip decreasing upward, the controlling fault terminates after cutting across the T3 surface, which has an age about 35.5 Ma. Several minor reverse faults with very limited displacement are developed in the anticline (Fig. 3).

The Eboliang No. 2 Anticline comprises two fault systems at different depths (Fig. 4). The upper system lies in a NE-vergent thrust-related fold and is dominated by a southwest dipping back thrust fault. The thrust fault is rooted at the UXG Fm., of late Eocene age, which is dominated by mudstone (Fig. 2). The lower system mainly comprises three high-angle reverse faults, forming a typical positive flower structure.

The Eboliang No. 3 Anticline can be subdivided into two fault systems (Fig. 5). The upper system lies within a fault-propagation fold and is dominated by a SW-dipping thrust fault, which is rooted in the UXG Fm.. The lower fault system is more complex. The deep anticline is mainly controlled by a NE-vergent thrust fault that terminates immediately after cutting across T2, which has an age of about 23.0 Ma. Four obvious minor reverse faults with different magnitudes of displacement are interpreted, and these faults totally modify the configuration of the deep anticline.

The Lenghu No. 4 Anticline is an asymmetric fold with a gentle west limb and relatively steep east limb (Fig. 6). It is mainly controlled by a west-dipping thrust fault that terminates in the LLH Formation, which is between about 53.5 and 43.8 Ma. This area experienced relatively rapid uplift, as there are exposures of E and W dipping strata of the XG Formation, of middle-late Eocene age, along the east limb of the structure.

Double fault systems are also obvious in seismic profiles that transect the Lenghu No. 5 and No. 6 anticlines, the structural architectures of which are very similar (Figs. 7 and 8). The shallow thrust-related folds are bounded by SW-dipping thrust faults, which are rooted within the UXG Formation. However, the fault throw indicated by the UXG and SG Formations in the Lenghu No.5 anticline is larger than that in the adjacent Lenghu No.6 anticline. The shallow anticlines are both modified in their geometry by displacement along back thrust faults. The lower systems comprise three high-angle reverse faults that merge together at depth, forming typical positive flower structures.

Two blind thrust faults, which root within basement rocks, control the geometry of the Lenghu No. 7 Anticline as a pop-up structure (Fig. 9). With the fault slip decreasing upward, the controlling faults terminate in the subsurface. Notably, several minor normal faults with

very limited displacement are developed in strata that define the crest of the fold.

5. Timing of deformation

5.1. Deformation at shallow crustal levels

Our interpretation of the high-resolution seismic profiles across structures in the western part of the NE Qaidam Basin provides a means of estimating the timing of shallow crustal deformation in the area by examining geometric relations displayed by sequences of Cenozoic growth strata. The ages of shallow sedimentary sequences containing growth strata have been sufficiently well-determined on the basis of fossil assemblages and magnetic polarity stratigraphy information (Fig. 2), as described above.

The Eocene LXG Formation (ca. 43.8 to 40.5 Ma) and overlying strata exposed in the Pingtai Uplift exhibit significant stratigraphic thinning towards the Saishiteng Shan (Fig. 10), and this relationship is interpreted to indicate that the tectonic activity initiated in the western part of the NE Oaidam Basin during the middle Eocene.

The lower Miocene XY Formation (ca. 23.0 to 15.3 Ma) in the Lenghu No. 4 and Eboliang No. 1 anticlines exhibits a modest amount of thinning towards the shallow anticline axes (Yin et al., 2019), which we interpret to reflect an early Neogene age of the initial deformation of these two structures.

According to the interpreted seismic cross-sections, the upper Miocene SY Formation (ca. 15.3 to 8.1 Ma) in the Lenghu No. 5 and Eboliang No. 2 anticlines exhibits a modest amount of thinning towards the shallow anticline axes (Figs. 4 and 5). And thinning pattern towards anticline core occurs about three hundred milliseconds above the topmost T2' reflector (ca. 15.3 Ma) in the Lenghu No. 5 Anticline (Fig. 7). Therefore, the shallow level deformation defining these folds was primarily occurred after the deposition of the Miocene SY Formation. (ca. 15.3 to 8.1 Ma).

Thinning pattern towards anticline core occurs about one hundred milliseconds above the topmost T1 reflector in the Lenghu No. 6 Anticline (Fig. 8). This geometric relation implies that this low amplitude anticline began to rise a bit following the deposition of the SZG Fm., and thus about 8 Ma.

As indicated by the 3-D seismic data, there are no obvious growth strata within the Cenozoic sedimentary sequence deformed in the

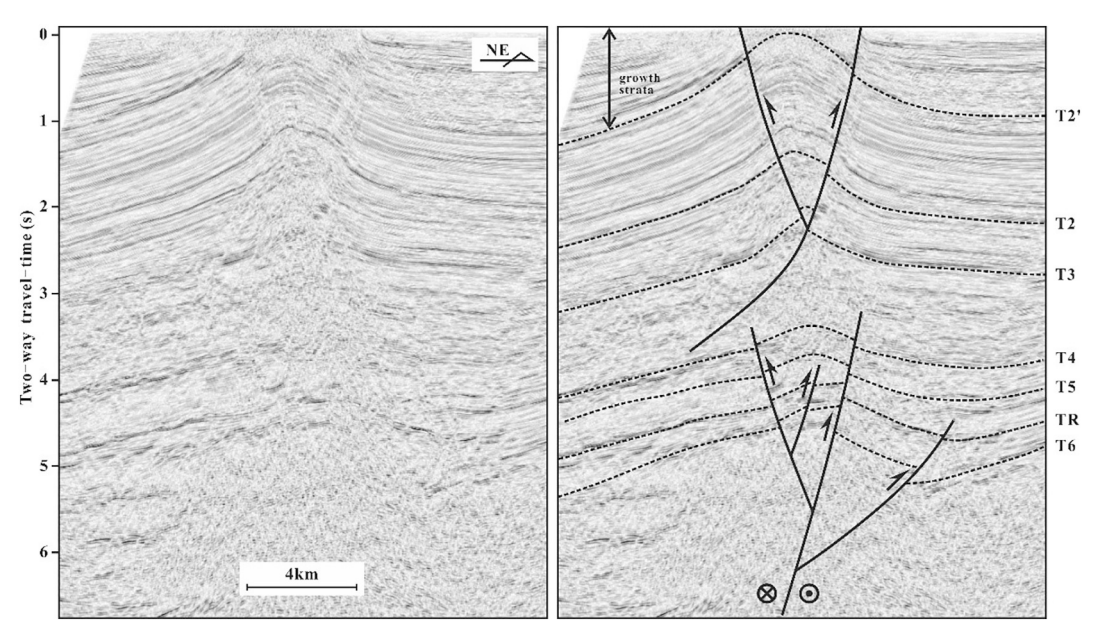


Fig. 4. Seismic cross section across the Eboliang No. 2 Anticline. (left) Original, (right), with structural interpretations. The location of profile is showed in Fig. 1b.

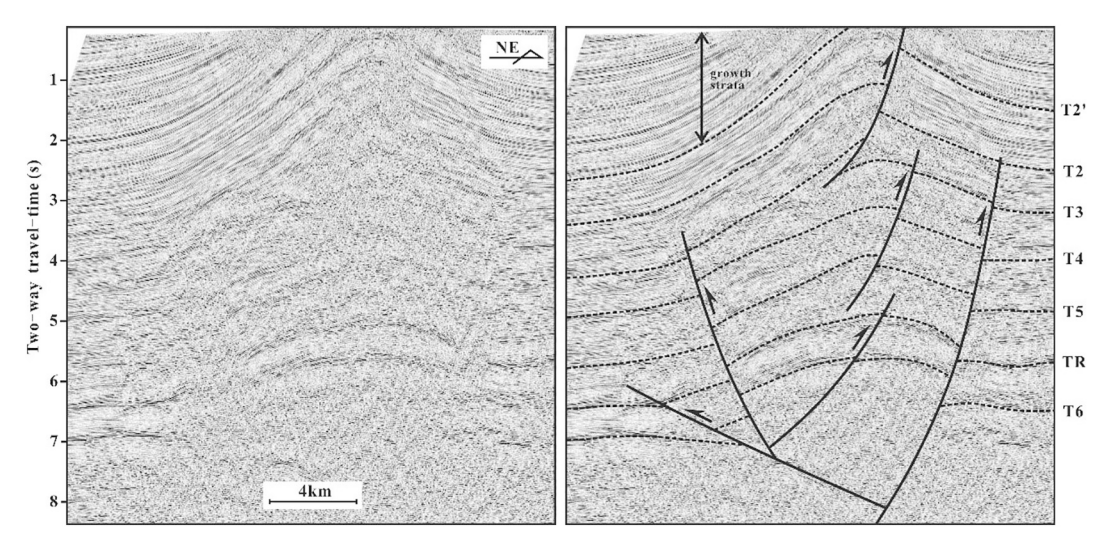


Fig. 5. Seismic cross section across the Eboliang No. 3 Anticline. (left) Original, (right), with structural interpretations. The location of profile is showed in Fig. 1b.

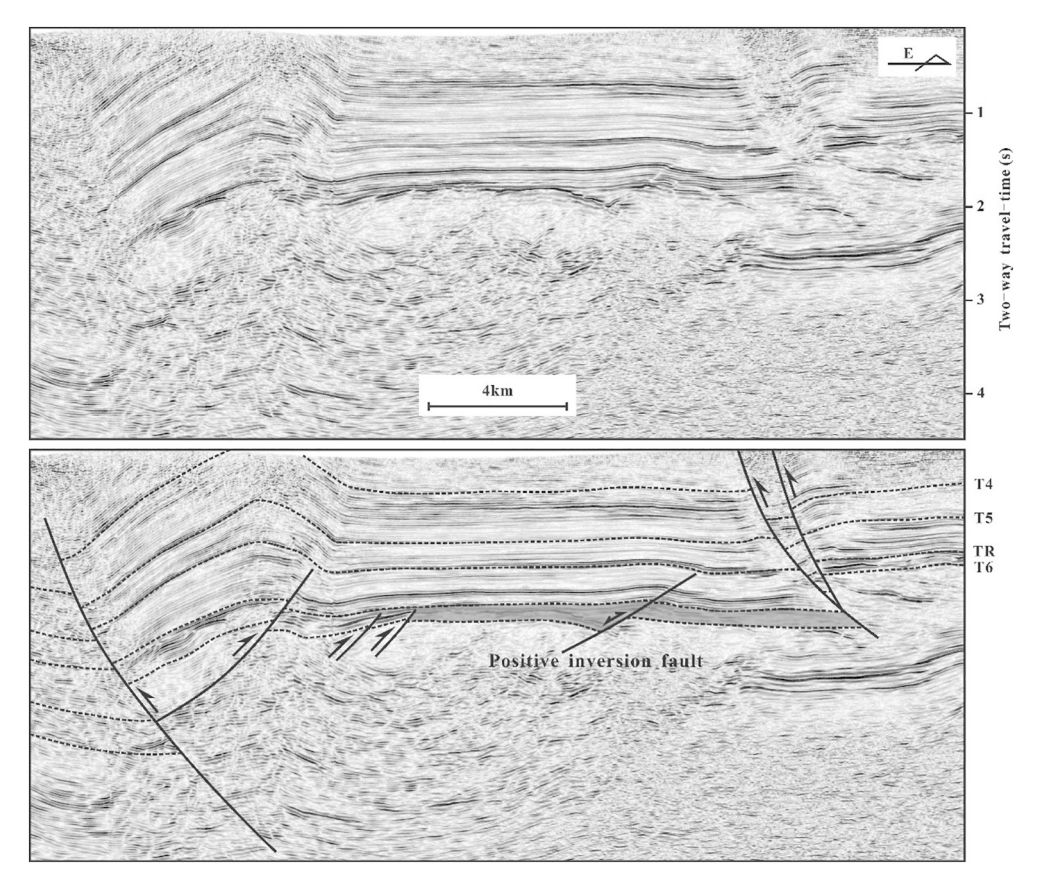


Fig. 6. Seismic cross section across the Lenghu No. 4 Anticline. (above) Original, (below), with structural interpretations. The location of profile is showed in Fig. 1b.

Lenghu No. 7 Anticline (Fig. 9). We thus speculate that this fold was formed in the Quaternary.

5.2. Deformation at deeper structural levels

In order to estimate the timing of deformation associated with fold development, we have restored the T5 surface in each of the structures, which are characterized by double fault systems at different structural levels, to a horizontal configuration, assuming that this surface, at the time of its formation was horizontal over the scale of the structures investigated. After the restoration of the T5 surface, which is the base of

the middle Eocene LXG Fm. and thus about 43.8 Ma, the Lenghu No. 5, Lenghu No. 6, Eboliang No. 2 and Eboliang No. 3 structures show that a phase of reverse faulting and folding had predated deposition of the LXG Fm. (Fig. 11). Therefore, we infer that deformation at deeper levels primarily initiated since the deposition of the lower to middle Eocene LLH Fm. (53.5–43.8 Ma).

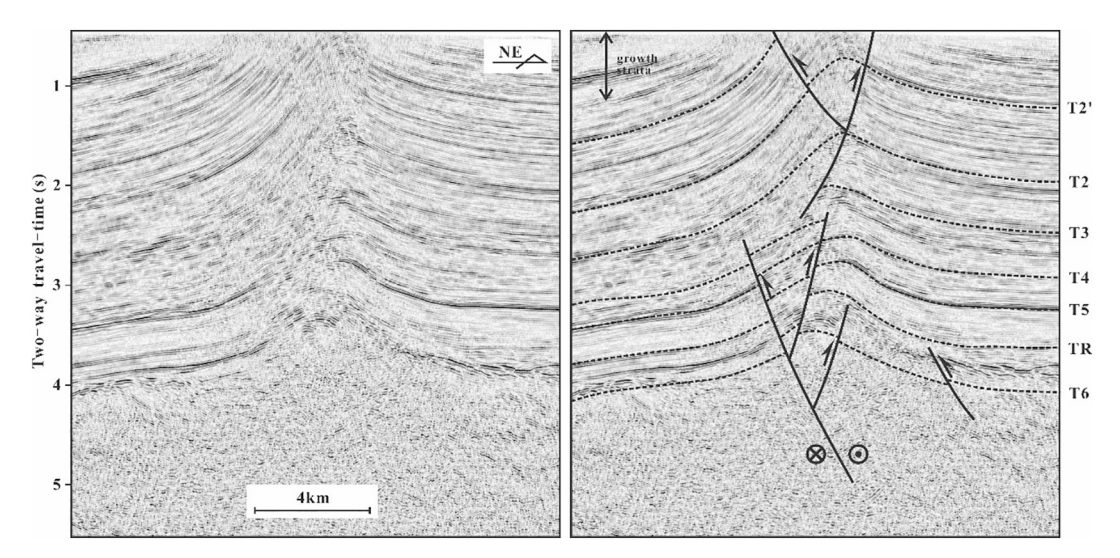


Fig. 7. Seismic cross section across the Lenghu No. 5 Anticline. (left) Original, (right), with structural interpretations. The location of profile is showed in Fig. 1b.

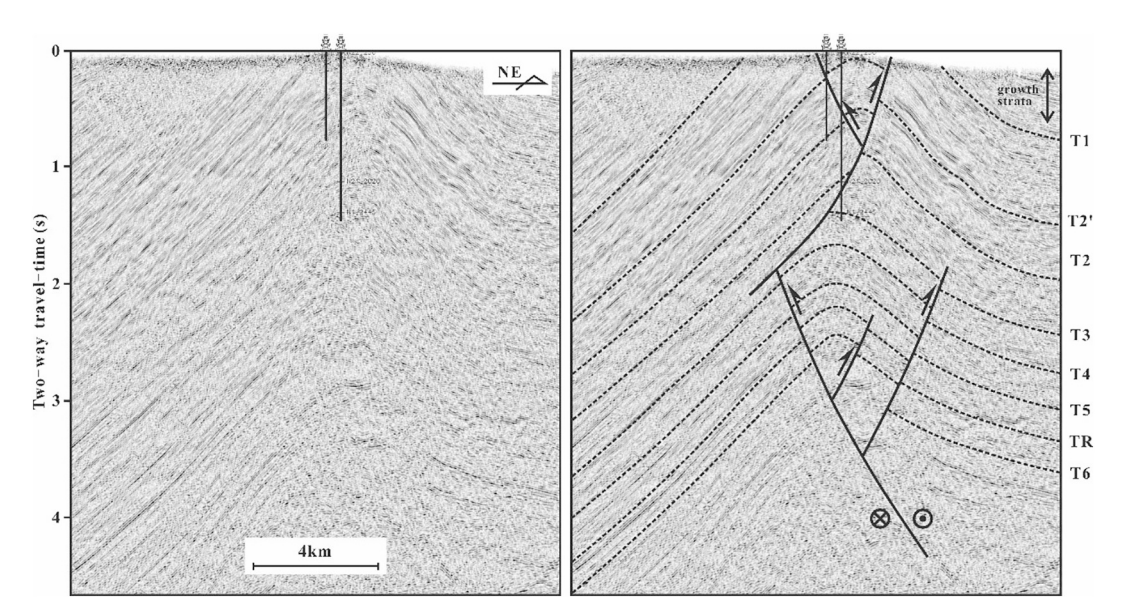


Fig. 8. Seismic cross section across the Lenghu No. 6 Anticline. (left) Original, (right), with structural interpretations. The location of profile is showed in Fig. 1b.

6. Discussion

6.1. Deformation mechanism

According to the surface and subsurface structural interpretations presented above, the Lenghu and Eboliang structural belts are characterized by double fault systems identified in seismic profiles approximately orthogonal to the trend of these belts, and also include normal faults associated with limited displacement within the very shallow levels of these structures and on their surface.

To explain these observations, we consider a transpressional deformation setting, comprising a lower transpressional fault system and an upper thrust-related fold set (Sylvester, 1988; Jamison, 1991; Tikoff and Peterson, 1998; Titus et al., 2007), which is similar to interpretations offered by workers studying the northwest part of the Qaidam Basin (Mao et al., 2016). The deeper fault systems involve high-angle positive flower structures in the Eboliang No. 2, Lenghu No. 5 and Lenghu No. 6 folds and these are geometrically consistent with deeper seated deformation, yet they still involve stratified materials, in this transpressional model. The upper thrust-related folds, and especially their near-surface

geology, were affected by transpressional deformation at lower crustal levels, and this ongoing, contemporary deformation is largely accommodated in terms of normal and strike-slip faults that extend to the anticline crests. We interpret these shallow brittle structures as extensional fractures (T fractures) or normal faults, which typically develop at orientations of about 45° to the principal strike-slip fault zone (Fig. 1c) (Sylvester, 1988). Trailing extensional imbricate fan structures may develop at the lateral fault tips (Fig. 1d) (Woodcock and Fischer, 1986). These faults are typically expressed as strike-slip faults on the surface, and usually have a dip-slip component. The left-step en echelon distribution of normal faults is interpreted to be consistent with a component of dextral shear along the deeper-seated fault systems (Campbell, 1959; Tikoff and Peterson, 1998).

6.2. Deformation phases

Several hypotheses have been put forward over the past few decades regarding the specific details of the Mesozoic history of the Qaidam Basin. Early researchers suggested that the basin initiated as a foreland basin (Hu et al., 1999; Jin et al., 1999; He et al., 2002; Yang et al., 2003,

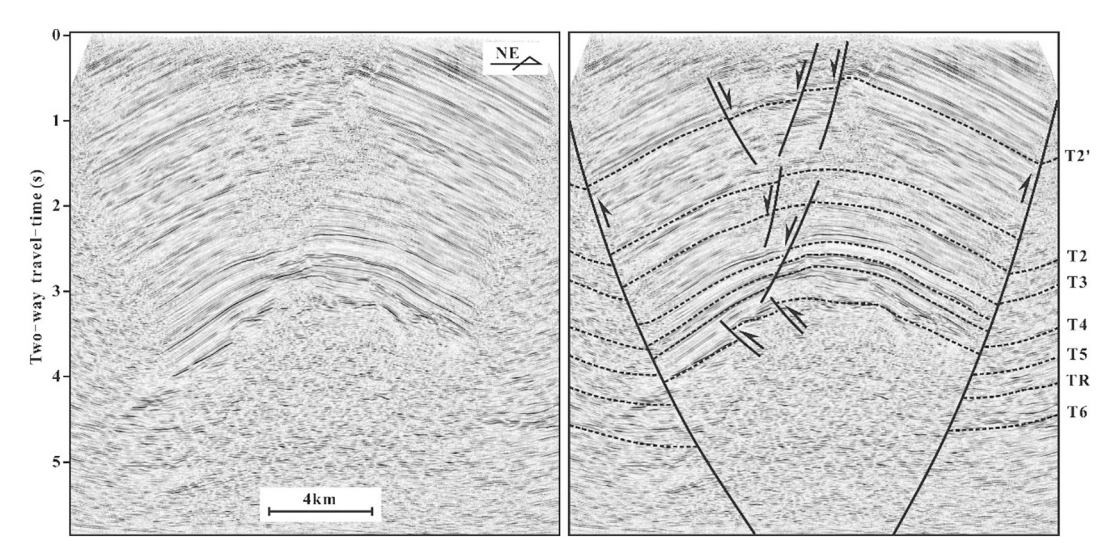


Fig. 9. Seismic cross section across the Lenghu No. 7 Anticline. (left) Original, (right), with structural interpretations. The location of profile is showed in Fig. 1b.

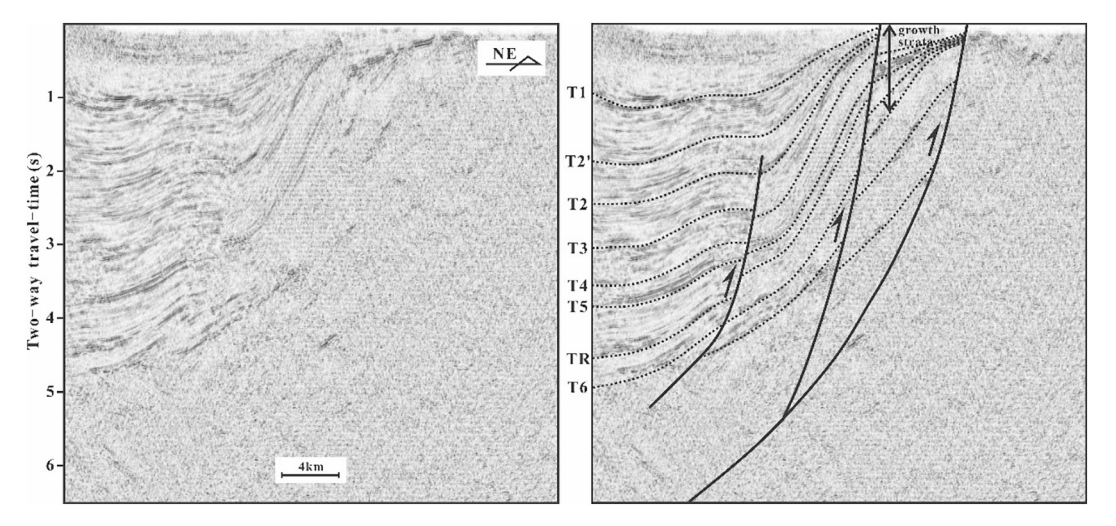


Fig. 10. Seismic cross section across the Pingtai Uplift. (left) Original, (right), with structural interpretations. The location of profile is showed in Fig. 1a.

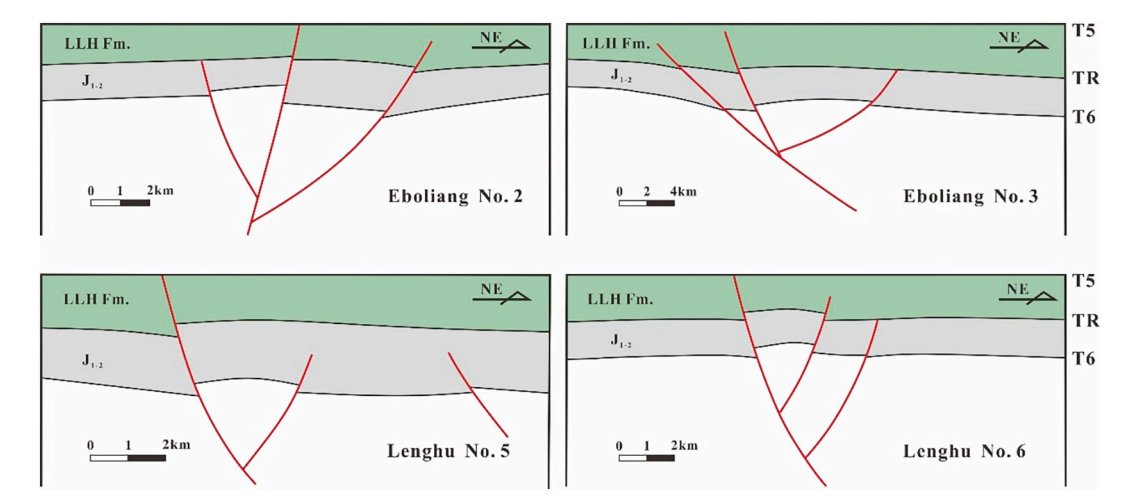


Fig. 11. Deep structural geometry of the main structures in the Eboliang and Lenghu structural belts after restoration of the T5 surface (the base of LXG Fm.) to the paleohorizontal. The original seismic cross sections of Eboliang No. 2, Eboliang No. 3, Lenghu No. 5 and Lenghu No. 6, are Fig. 4, Fig. 5, Fig. 7 and Fig. 8, respectively.

2004). However, based on interpretations of seismic profiles and provenance analysis, the Qaidam Basin was interpreted by several workers to have formed as an extensional depression or rift basin during the Early Jurassic to the Early Cretaceous (Gao et al., 2003; Liu et al., 2004; Duan et al., 2007; Luo, 2008; Lou et al., 2009; Wu et al., 2011; Cheng et al., 2019a; Zhao et al., 2020). Subsurface information based on drilling experiments and seismic data show that Jurassic strata were chiefly deposited in the northern and western parts of the Qaidam Basin (GMBQP, 1991; Fu et al., 2014). The coal-bearing strata and mudstones of inferred lacustrine facies of Early to Middle Jurassic age typically are good source rocks in the basin. A small number of normal faults were active in the western part of the NE Qaidam Basin during the Early to Middle Jurassic (Zhao et al., 2020) and we regard this period of Mesozoic extension as the first deformation phase in the region that is now occupied by the western part of the NE Qaidam Basin.

On the basis of the restoration of the T5 surface (the base of the LXG Fm.) to the paleohorizontal, the phase of shortening that resulted in the anticlines situated at deeper structural levels first began during the deposition of the LLH Fm., between about 54 and 44 Ma in some of the local structures (e.g., Eboliang No. 2, Eboliang No. 3, Lenghu No. 5 and Lenghu No. 6 folds) (Fig. 11). This observation is broadly consistent with the work of Bush et al. (2016), studying surface exposures in the Dahonggou anticline area (DHG) (Fig. 1a). These workers reported a change in sediment provenance from a late Paleocene to early Eocene derivation from Permian and Triassic arc rocks exposed along the southern to southwestern margins of the Qaidam Basin to an Eocene to Oligocene derivation from lower Paleozoic and Mesozoic crystalline rocks exposed in the central to northern Qilian Shan and Nan Shan. This early phase of shortening was associated with the reactivation of preexisting normal faults in some areas of the Lenghu and Eboliang structural belts, thus forming the positive inversion structures that are readily identified in some of the seismic profiles (Fig. 6). The onset of contractional deformation in the broad area of the western part of the NE Qaidam Basin occurred during the deposition of the middle Eocene LXG Fm., thus beginning at about 43.8 Ma. Fold development at shallower structural levels throughout the area began gradually following the deposition of the lower Miocene XY Fm., and thus after about 23.0 Ma. We regard this continuity of crustal shortening since the early Cenozoic as the second deformation phase affecting the western part of the NE Qaidam Basin. This observation is also consistent with the results of the study of Bush et al. (2016), who recognized an early to middle Miocene source change along the frontal Nan Shan and North Qaidam thrust belt.

The third and ongoing (contemporary) deformation phase in the western part of the NE Qaidam Basin has involved the development of a dextral transpressional system characterized by the formation of positive flower structures at lower structural levels and en echelon distributed normal faults on the surface. This style of deformation is also observed in some SE-trending fold belts located in the northwest part of the Qaidam Basin (Mao et al., 2016). Each belt consists of several right-stepping en echelon anticlines with numerous normal and strike-slip faults crossing their crests. Growth strata indicate that the dextral transpressional deformation within the northern Qaidam Basin probably developed since the deposition of the Miocene SZG Fm., and thus after about 8.1 Ma (Mao et al., 2016).

6.3. Implications for the growth of the Tibetan Plateau

The history of the growth of the Tibetan Plateau is one of the key issues for ongoing geologic research (Yin et al., 2008a). Several researchers have proffered the argument that the plateau progressively grew from south to north, and that the northern Tibetan Plateau, including the Qaidam Basin, did not experience any deformation until beginning in the middle to late Miocene (Molnar and Tapponnier, 1975; Métivier et al., 1998; Meyer et al., 1998; Tapponnier et al., 2001; Lu and Xiong, 2009). Contrasting viewpoints center around the argument that

deformation induced by the Indo-Asian collision occurred across the modern Tibetan Plateau during or soon after the onset of collision (Burg et al., 1994; Jolivet et al., 1999, 2001; Yin et al., 2007, 2008a, 2008b; Zheng et al., 2010; Zhuang et al., 2011; Liu et al., 2013; Yuan et al., 2013; Li et al., 2014; Yu et al., 2014b, 2017; Cheng et al., 2019b).

In recent years, Qinghai Oilfield, PetroChina, has carried out petroleum exploration in many parts of the Qaidam Basin and obtained abundant drill core and logging data from hundreds of wells, as well as abundant seismic data throughout the basin. Based on the thicknessdistribution maps of Cenozoic strata from Yin et al. (2008b), combined with some new wells and seismic data, we have assembled seven stratigraphic isopach maps of the basin that facilitate analysis of the Cenozoic evolution of the pattern of crustal shortening across the Qaidam Basin (Fig. 12).

The east-west extent of the early to middle Eocene Qaidam Basin was much smaller than (about 50% of) its present size. As shown on the isopach map (Fig. 12a), the Qaidam Basin was not a symmetric basin during the deposition of the lower Eocene Lulehe Formation. Its main depocenter, located around the Yiliping area in the northeast part of the basin, is close to the Oilian Shan. Several smaller depocenters were scattered in the northeastern and western basin, along the Oilian Shan and Oimen Tagh Range respectively (Fig. 12a). Based on flexural modeling, Cheng et al. (2019b) considered that the topographic load generated by both the Qimen Tagh Range and the Qilian Shan was responsible for the subsidence of the Qaidam Basin during this time interval. These NW-trending depocenters may reflect a NE-SW oriented compressional stress regime, which resulted in the formation of the deep positive inversion structures in the western part of the NE Qaidam Basin (Fig. 13a). The sedimentologic characteristics of the LLH Fm., of early Eocene age, include a thick sequence of coarse conglomerates in the lower part of the formation, with detritus mainly derived from the Qilian Shan and Qimen Tagh Range, and we interpret these strata to record the initial growth of the northern Tibetan Plateau (Fig. 2). Therefore, the far-field effects of the Indo-Asian collision had, by the early Eocene, considerable influence on the area of the Qimen Tagh Range and Qilian Shan. These geologic observations support the hypothesis that the Tibetan Plateau did not experience a simple northward growth progression (Yin et al., 2008a), and instead, the deformation induced by the Indo-Asian collision affected much of the present extent of the Tibetan Plateau during or soon after the onset of collision.

Although the extent of the Qaidam Basin was enlarged gradually between the time period of the deposition of the LXG Fm. to the XY Fm. (ca. 43.8 to ca. 15.3 Ma, from the middle Eocene to the middle Miocene), the configuration of the basin during this time is similar to the time interval of deposition of the LLH Formation in the early Eocene, between about 53.5 and 43.8 Ma. The largest depocenter, located around the Yiliping area in the northeast part of the basin, as well as some minor depocenters along the eastern Qimen Tagh Range and Qilian Shan, were still expanding in a NW-SE direction (Fig. 12b, c, d and e) and we interpret this observation to reflect sustained compression and continued uplift of the Qilian Shan and Qimen Tagh Range. Notably, all of the deep shortening-related structures as well as shallow anticlines in the western part of the NE Qaidam Basin were initially developed during this time period (Fig. 13a).

Concurrent with the deposition of the SY and SZG formations, between about 15.3 and 2.5 Ma, from the middle Miocene into the earliest Quaternary, the isopach data show one notable feature in that some depocenters shifted from a NW-SE to a more WNW-ESE orientation, especially the major depocenter located around the Yiliping area in the northeast part of the basin (Fig. 12f and g). This change in orientation implies a change in compressional stress direction after the middle Miocene (Fig. 12f and g). Based on paleomagnetic data, provenance analysis and seismic interpretation, recent studies show that rapid strike-slip displacement along the ATF also began in the middle Miocene (Wu et al., 2012, 2019; Li et al., 2017; Zhang et al., 2018). Magnetic fabric data, as anisotropy of magnetic susceptibility results, from both

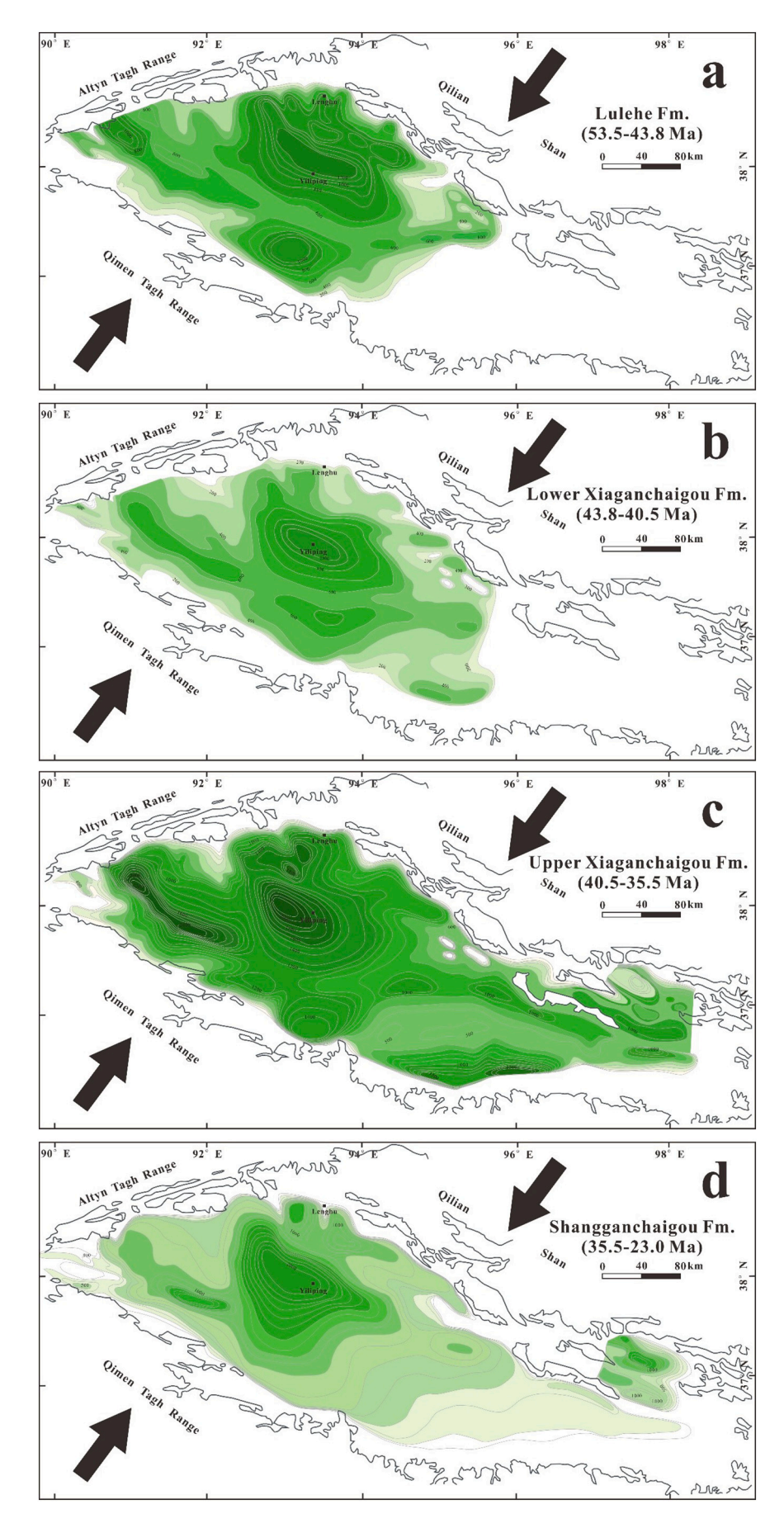
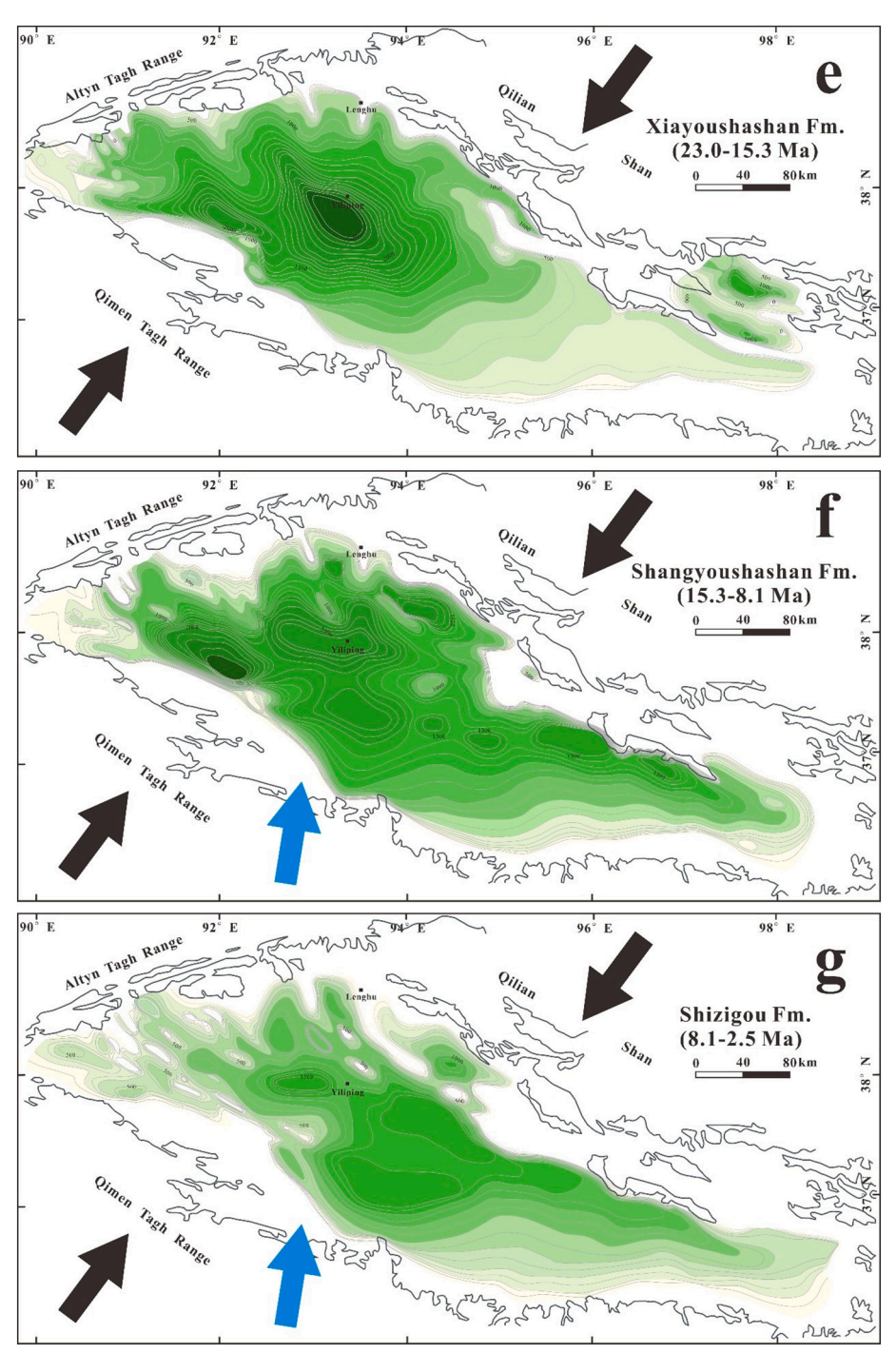


Fig. 12. (a) Isopach map of the Lulehe Formation (ca. 53.5–43.8 Ma). (b) Isopach map of the Lower Xiaganchaigou Formation (ca. 43.8–40.5 Ma). (c) Isopach map of the Upper Xiaganchaigou Formation (ca. 40.5–35.5 Ma). (d) Isopach map of the Shangganchaigou Formation (ca. 35.5–23.0 Ma). (e) Isopach map of the Xiayoushashan Formation (ca. 23.0 to 15.3 Ma). (f) Isopach map of the Shangyoushashan Formation (ca. 15.3 to 8.1 Ma). (g) Isopach map of the Shizigou Formation (ca. 8.1–2.5 Ma).

Fig. 12. (continued).



the XG Fm. and XY Fm. strata exposed in the Eboliang No. 1 Anticline were interpreted to support a NNE-SSW principal stress orientation (Yu et al., 2014a), which is inconsistent with the modern NNW-SSE fold trends. Furthermore, paleomagnetic data from the same rock sequences indicate no significant rotation of the Qaidam Basin during the Neogene (Dupont-Nivet et al., 2002; Yu et al., 2014b). Therefore, we suggest that the NNE-directed compressional stress led to rapid left-lateral strike-slip displacement along the ATF following the deposition of the SY Fm. (Fig. 13b). South of the ATF, there also exists a series of orocline-like arcuate structures, such as the Akatengnengshan and Youshashan anticlines, that extend from the Qilianshan to the east and Qimen Tagh to the west. These features are characterized by a change in strike from NW-SE far south of the ATF to nearly E-W close to the fault (< ~60 km)

(Li et al., 2017). According to interpretations from several paleomagnetic studies, frictional drag associated with sinistral strike-slip motion of the ATF likely resulted in the counterclockwise rotation, by up to 50 degrees, of some of these anticline structures (Rumelhart et al., 1999; Chen et al., 2002; Li et al., 2017) (Fig. 13b). In our study area, dextral strike-slip deformation in the western part of the NE Qaidam Basin is interpreted to have resulted from the NNE-directed compressional stress, which was developed since the deposition of the SZG Fm., and thus after about 8.1 Ma (Fig. 13c). The characteristic structural pattern of double fault systems in the anticlines of the western part of the NE Qaidam Basin is interpreted as the superimposed result of the NE-SW and NNE-SSW compression.

In addition to the development of the several very distinctive

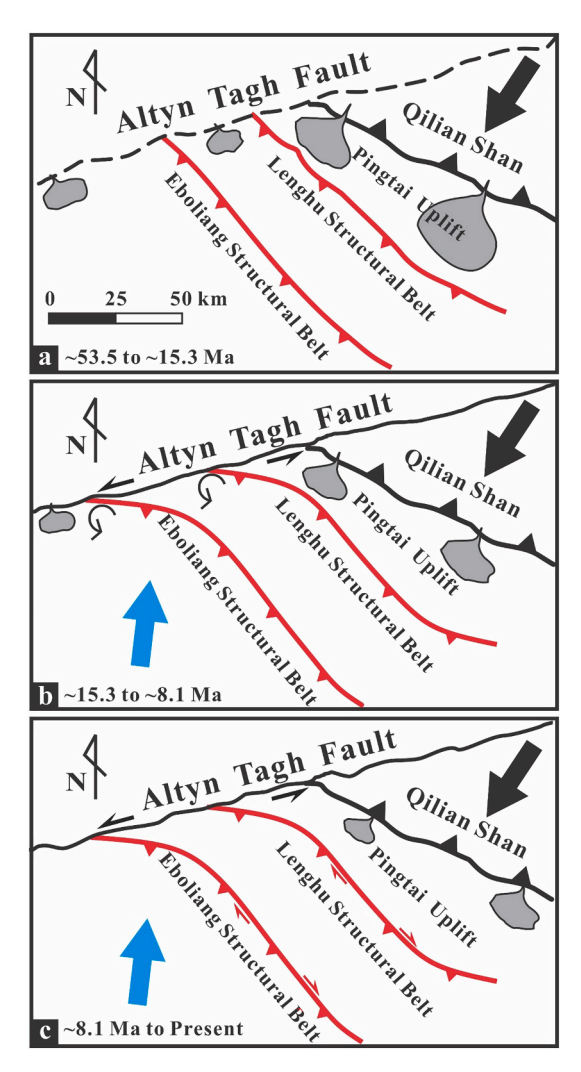


Fig. 13. Schematic tectonic evolution model of the western part of the NE Qaidam Basin and its surrounding areas. (a) early Eocene to mid-Miocene time: early response to the initial Indo-Asian "hard" collision, with a regional NE-SW compressional stress state associated with northeast-directed thrusting of the Qilian Shan, resulting in the initial development of thrusts and folds in the western part of the NE Qaidam Basin between 53.5 and 15.3 Ma. (b) middle Miocene to latest Miocene time: response to the growth of the Tibetan Plateau, with NNE-SSW directed compressional stress resulting in enhanced left-lateral strike-slip displacement along the ATF and subsequent counterclockwise rotation, by up to 50 degrees, of some anticlines south of the fault between ca. 15.3 and 8.1 Ma. (c) Pliocene to today: NNE-SSW compressional stress results in focused dextral transpressional deformation in the Lenghu and Eboliang structural belts since ca. 8.1 Ma.

anticlines in the western part of the NE Qaidam Basin, the onset of deformation in the Yingxiongling Structure Belt, located in the western Qaidam Basin, took place during the middle Miocene (Yu et al., 2011; Cheng et al., 2018; Huang et al., 2020; Wang et al., 2020; Wu et al., 2020). The Nanyishan Anticline is interpreted as a transpressive structure, and the initiation of its development took place in the late Miocene (Liu et al., 2017). The lower parts of the Honggouzi, Jiandingshan, Dafengshan and Jianshan anticlines are generally characterized by typical positive flower structures related to a dextral transpressional fault system, which initiated in the middle Miocene and the rate of deformation accelerated in the late Miocene (Mao et al., 2016). The middle-late Miocene initiation of the strike-slip deformation within the entire northern Qaidam Basin, including along the ATF, is best interpreted as being an integral part of the pulsed growth of the entire Tibetan Plateau during that time (Blisniuk et al., 2001; Clark et al., 2005;

Molnar, 2005).

7. Conclusion

Using surface geology, seismic reflection data and basin-wide isopach maps, all presented in this paper, we provide a synthesis of the structural deformation pattern and the timing of deformation of the western part of the NE Qaidam Basin and propose a mechanism of formation of the structural features during the middle Mesozoic through Cenozoic time that is consistent with all available data. There are two key conclusions that can be derived from our work. First, the many anticlines in the Lenghu and Eboliang structural belts of the western part of the NE Qaidam Basin are characterized by double fault systems at different structural levels. The shallower thrust fault system is typically detached within mudstone dominated intervals in the late Eocene UXG Fm., while the deeper-seated dextral transpressional fault system is characterized by positive flower structures. Second, contractional deformation initially occurred in the western part of the NE Qaidam Basin during the early Eocene, based on restoration of the T5 surface, of middle Eocene age, to the paleohorizontal, and we interpret this deformation as an early, far-field effect of the Indo-Asian "hard" collision (Van Hinsbergen et al., 2012). The compressional stress trajectory has changed orientation to an NNE direction since the middle Miocene, and this resulted in the initiation of rapid left-lateral strike-slip displacement along the ATF and dextral transpressional deformation in the western part of the NE Qaidam Basin. This phase of deformation also represents an integral part of the pulsed growth of the Tibetan Plateau as a whole.

Declaration of Competing Interest

The authors declare that they have no known competing financial interests or personal relationships that could have appeared to influence the work reported in this paper.

Acknowledgements

This work is financially supported by Petrochemical Fund Project of National Natural Science Foundation of China (No. U1663203) and Science Foundation of China University of Petroleum, Beijing (No. ZX20150066). The study is also financially sponsored by the foundation of State Key Laboratory of Petroleum Resources and Prospecting, China University of Petroleum (Beijing) (No. PRP/indep–2–1501). We thank Qinghai Oilfield Company, PetroChina for providing seismic reflection profiles and isopach maps.

References

Bian, Q., Zhang, D.W., Yu, X.J., Cheng, X., Du, W., Liu, R.C., Wang, Z.D., Guo, Z.J., 2019. Transpressional salt tectonic system in western Qaidam Basin, Western China. AAPG Bull. 103, 547–568.

Blisniuk, P.M., Hacker, B.R., Glodny, J., Ratschbacher, L., Bi, S., Wu, Z., McWilliams, M. O., Calvert, A., 2001. Normal faulting in central Tibet since at least 13.5 Myr ago. Nature 412, 628–632.

Bovet, P.M., Ritts, B.D., Gehrels, G., Abbink, A.O., Darby, B., Hourigan, J., 2009. Evidence of Miocene crustal shortening in the north Qilian Shan from Cenozoic stratigraphy of the western Hexi Corridor, Gansu Province, China. Am. J. Sci. 309 (4), 290–329.

Burchfiel, B.C., Deng, Q.D., Molnar, P., Royden, L., Wang, Y.P., Zhang, P.Z., Zhang, W.Q., 1989. Intracrustal detachment within zones of continental deformation. Geology 17 (8), 748–752.

Burg, J.P., Davy, P., Martinod, J., 1994. Shortening of analogue models of the continental lithosphere: new hypothesis for the formation of the Tibetan plateau. Tectonics 13 (2), 475–483.

Bush, M.A., Saylor, J.E., Horton, B.K., Nie, J., 2016. Growth of the Qaidam Basin during Cenozoic exhumation in the northern Tibetan Plateau: inferences from depositional patterns and multiproxy detrital provenance signatures. Lithosphere 8 (1), 58–82. Campbell, J.D., 1959. En echelon folding. Econ. Geol. 54, 505–509.

Chen, Z.L., Zhang, Y.Q., Wang, X.F., Chen, X.H., 2001. Fission track dating of apatite constrains on the Cenozoic uplift of the Altyn Tagh Mountain. Acta Geosci. Sin. 22 (5), 413–418 (In Chinese with English abstract).

Chen, Y., Gilder, S., Halim, N., Cogné, J.P., Courtillot, V., 2002. New paleomagnetic constraints on central Asian kinematics: displacement along the Altyn Tagh fault and rotation of the Qaidam Basin. Tectonics 21 (5), 1042.

- Chen, Z., Wang, X.F., Yin, A., Chen, B.L., Chen, X.H., 2004. Cenozoic left-slip motion along the central Altyn Tagh Fault as inferred from the sedimentary record. Int. Geol. Rev. 46, 839–856.
- Cheng, F., Jolivet, M., Fu, S., Zhang, Q., Guan, S., Yu, X., Guo, Z., 2014. Northward growth of the Qimen Tagh Range: a new model accounting for the Late Neogene strike-slip deformation of the SW Qaidam Basin. Tectonophysics 632, 32–47.
- Cheng, F., Guo, Z.J., Jenkins, H.S., Fu, S.T., Cheng, X., 2015a. Initial rupture and displacement on the Altyn Tagh fault, northern Tibetan Plateau: constraints based on residual Mesozoic to Cenozoic strata in the western Qaidam Basin. Geosphere 11, 921–942
- Cheng, X., Fu, S.T., Wang, H.F., Yu, X.J., Cheng, F., Liu, R.C., Du, W., Guo, Z.J., 2015b. Geometry and kinematics of the Arlar strike-slip fault, SW Qaidam basin, China: new insights from 3-D seismic data. J. Asian Earth Sci. 98, 198–208.
- Cheng, F., Jolivet, M., Fu, S.T., Zhang, C.H., Zhang, Q.Q., Guo, Z.J., 2016. Large-scale displacement along the Altyn Tagh Fault (North Tibet) since its Eocene initiation: insight from detrital zircon U-Pb geochronology and subsurface data. Tectonophysics 677, 261-270
- Cheng, X., Zhang, Q.Q., Yu, X.J., Du, W., Liu, R.C., Bian, Q., Wang, Z.D., Zhang, T., Guo, Z.J., 2017. Strike-slip fault network of the Huangshi structure, SW Qaidam Basin: insights from surface fractures and seismic data. J. Struct. Geol. 94, 1–12.
- Cheng, X., Zhang, D.W., Jolivet, M., Yu, X.J., Du, W., Liu, R.C., Guo, Z.J., 2018. Cenozoic structural inversion from transtension to transpression in Yingxiong Range, western Qaidam Basin: new insights into strike-slip superimposition controlled by Altyn Tagh and eastern Kunlun Faults. Tectonophysics 723, 229–241.
- Cheng, F., Jolivet, M., Guo, Z.J., Lu, H.Y., Zhang, B., Li, X.Z., Zhang, D.W., Zhang, C.H., Zhang, H.Z., Wang, L., Wang, Z.Q., Zhang, Q.Q., 2019a. Jurassic-Early Cenozoic tectonic inversion in the Qilian Shan and Qaidam Basin, North Tibet: new insight from seismic reflection, isopach mapping, and drill core data. J. Geophys. Res. Solid Earth 124, 12077–12098.
- Cheng, F., Garzione, C.N., Jolivet, M., Guo, Z.J., Zhang, D.W., Zhang, C.H., Zhang, Q.Q., 2019b. Initial deformation of the Northern Tibetan Plateau: insights from deposition of the Lulehe Formation in the Qaidam Basin. Tectonics 38 (1–2), 741–766.
- Chinese State Bureau of Seismology, 1992. The Altyn Tagh Active Fault System (in Chinese). Seismology Publishing House, Beijing, pp. 1–319.
- Clark, M.K., 2012. Continental collision slowing due to viscous mantle lithosphere rather than topography. Nature 483 (7387), 74–77.
- Clark, M.K., House, M.A., Royden, L.H., Whipple, K.X., Burchfiel, B.C., Zhang, X.,
 Tang, W., 2005. Late Cenozoic unlift of southeastern Tibet. Geology 33, 525–528.
- Clark, M.K., Farley, K.A., Zheng, D., Wang, Z., Duvall, A.R., 2010. Early Cenozoic faulting of the northern Tibetan Plateau margin from apatite (U-Th)/He ages. Earth Planet. Sci. Lett. 296 (1–2), 78–88.
- Dayem, K.E., Molnar, P., Clark, M.K., Houseman, G.A., 2009. Far-field lithospheric deformation in Tibet during continental collision. Tectonics 28 (6), 1–9.
- Delville, N., Arnaud, N., Montel, J.M., Roger, F., Brunel, M., Tapponnier, P., Sobel, E., 2001. Paleozoic to Cenozoic deformation along the Altyn Tagh fault in the Altun Shan massif area, eastern Qilian Shan, northeastern Tibet, China. Geol. Soc. Am. Mem. 194, 269–292.
- Du, W., Zhang, D.W., Yu, X.J., Cheng, X., Wang, Z.D., Bian, Q., Guo, Z.J., 2019. Relationship between the Altyn Tagh strike-slip fault and the Qaidam Basin: new insights from superposed buckle folding in Hongsanhan. Int. Geol. Rev. 1, 1–11.
- Duan, H.L., Zhong, J.H., Ma, F., Zhang, Y.Z., Li, Y., Wen, Z.F., 2007. Prototypes and evolution of the Mesozoic basin in Western Qaidam. Acta Geosci. Sin. 4, 356–368 (In Chinese with English abstract).
- Dupont-Nivet, G., Butler, R.F., Yin, A., Chen, X., 2002. Paleomagnetism indicates no Neogene rotation of the Qaidam Basin in northern Tibet during Indo-Asian Collision. Geology 30 (3), 263–266.
- Dupont-Nivet, G., Robinson, D., Butler, R.F., Yin, A., Melosh, H.J., 2004. Concentration of crustal displacement along a weak Altyn Tagh Fault: evidence from paleomagnetism of the northern Tibetan Plateau. Tectonics 23, 1020.
- Dupont-Nivet, G., Lippert, P.C., Van Hinsbergen, D.J.J., Meijers, M.J.M., Kapp, P., 2010.
 Palaeolatitude and age of the Indo-Asia collision: palaeomagnetic constraints.
 Geophys. J. Int. 182 (3), 1189–1198.
- Duvall, A.R., Clark, M.K., van der Pluijm, B.A., Li, C., 2011. Direct dating of Eocene reverse faulting in northeastern Tibet using Ar-dating of fault clays and lowtemperature thermochronometry. Earth Planet. Sci. Lett. 304 (3–4), 520–526.
- Fang, X., Zhao, Z., Li, J., Yan, M., Pan, B., Song, C., Dai, S., 2005. Magnetostratigraphy of the late Cenozoic Laojunmiao anticline in the northern Qilian Mountains and its implications for the northern Tibetan Plateau uplift. Sci. China Earth Sci. 48 (7), 1040–1051.
- Fang, X.M., Zhang, W.L., Meng, Q.Q., Gao, J.P., Wang, X.M., King, J., Song, C.H., Dai, S., Miao, Y.F., 2007. High-resolution magnetostratigraphy of the Neogene Huaitoutala section in the eastern Qaidam Basin on the NE Tibetan Plateau, Qinghai Province, China and its implication on tectonic uplift of the NE Tibetan Plateau. Earth Planet. Sci. Lett. 258, 293–306.
- Fu, S.T., Yuan, J.Y., Wang, L.Q., Zhang, S.C., 2014. Study on Hydrocarbon Geological Reservoir-Forming Conditions in Qaidam Basin. Science Publishing House, p. 466 (In Chinese).
- Fu, S., Ma, D., Guo, Z.J., Cheng, F., 2015. Strike-slip superimposed Qaidam Basin and its control on oil and gas accumulation, NW China. Pet. Explor. Dev. 42, 778–789.
- Gao, X.Z., Chen, F.J., Ma, D.D., Wang, L.Q., Liu, Z., 2003. Tectonic evolution of the northern Qaidam Basin during Mesozoic and Cenozoic eras. Northwest. Geol. 36 (4), 16–23 (In Chinese with English abstract).

Gao, J., Li, S., Dai, S., Li, A., Peng, Y., 2009. Constraints of tectonic evolution in provenance from detrital zircon fission-track data of Cenozoic strata of Xichagou district in western Qaidam basin. J. Lanzhou Univ. 45, 1–7 (In Chinese with English abstract)

- Garzanti, E., Van Haver, T., 1988. The indus clastics: forearc basin sedimentation in the Ladakh Himalaya (India). Sediment. Geol. 59 (3–4), 237–249.
- Gehrels, G.E., Yin, A., Wang, X.F., 2003. Detrital-zircon geochronology of the northeastern Tibetan plateau. Geol. Soc. Am. Bull. 115 (7), 881–896.
- GMBQP (Geology and Mineral Bureau of the Qinghai Province), 1991. Regional Geology of Qinghai Province. Geological Publishing House, Beijing, p. 662 (in Chinese).
- Green, O.R., Searle, M.P., Corfield, R.I., Corfield, R.M., 2008. Cretaceous-Tertiary carbonate platform evolution and the age of the India-Asia collision along the Ladakh Himalaya (Northwest India). J. Geol. 116 (4), 331–353.
- He, Z.H., Liu, Z.J., Guo, W., Dong, Q.S., 2002. The genetic type of the Mesozic basin in northern Qaidam and its tectonic-sedimentary evolution. J. Jilin Univ. (Earth Sci. Ed.) 32 (4), 92–100 (In Chinese with English abstract).
- Hu, S.Q., Cao, Y.J., Huang, J.X., Mou, Z.H., 1999. Discussion on formation and evolution of Jurassic basin-prototype of Qaidam Basin. Exp. Petrol. Geol. 21 (3), 189–192 (In Chinese with English abstract).
- Hu, X., Garzanti, E., Moore, T., Raffi, I., 2015. Direct stratigraphic dating of India-Asia collision onset at the Selandian (middle Paleocene, 59±1 Ma). Geology 43 (10), 859–862.
- Hu, X., Wang, J., BouDagher-Fadel, M., Garzanti, E., An, W., 2016. New insights into the timing of the India-Asia collision from the Paleogene Quxia and Jialazi formations of the Xigaze forearc basin, South Tibet. Gondwana Res. 32, 76–92.
- Huang, W., Hinsbergen, D.J., Lippert, P.C., Guo, Z., Dupont-Nivet, G., 2015.
 Paleomagnetic tests of tectonic reconstructions of the India-Asia collision zone.
 Geophys. Res. Lett. 42, 2642–2649.
- Huang, K., Wu, L., Zhang, J.Y., Zhang, Y.S., Xiao, A.C., Lin, X.B., Wang, L.Q., Chen, H.L., 2020. Structural coupling between the Qiman Tagh and the Qaidam Basin, northern Tibetan Plateau: a perspective from the Yingxiong Range by integrating field mapping, seismic imaging, and analogue modeling. Tectonics 39. https://doi.org/ 10.1029/2020TC006287 e2020TC006287.
- Hubbard, J., Shaw, J.H., 2009. Uplift of the Longmen Shan and Tibetan plateau, and the 2008 Wenchuan (M=s7.9) earthquake. Nature 458, 194–197.
- Huo, G.M., 1990. Petroleum Geology of China: Oil Fields in Qinghai and Xizang. Chinese Petroleum Industry Press, Beijing, p. 483 (in Chinese).
- Jamison, W.R., 1991. Kinematics of compressional fold development in convergent wrench terrances. Tectonophysics 190, 209–232.
- Jia, D., Wei, G., Chen, Z., Li, B., Zeng, Q., Yang, G., 2006. Longmen Shan fold-thrust belt and its relation to the western Sichuan Basin in central China: new insights from hydrocarbon exploration. AAPG Bull. 90, 1425–1447.
- Jin, J.Q., Zhao, W.Z., Xue, L.Q., Meng, Q.R., 1999. Prototype and evolution of Jurassic basins in NW China. Geol. Rev. 45 (1), 92–100 (In Chinese with English abstract).
- Jolivet, M., Roger, F., Arnaud, N., Brunel, M., Tapponnier, P., Seward, D., 1999. Histoire de l'exhumation de l'Altun Shan: indications sur l'age de la subduction du bloc du Tarim sous le système de l'Altyn Tagh (Nord Tibet). Comp. Rend. Acad. Sci. 329 (10) 749-755
- Jolivet, M., Brunel, M., Seward, D., Xu, Z.Q., Yang, J.S., Roger, F., Tapponnier, P., Malavieille, J., Arnaud, N., Wu, C., 2001. Mesozoic and Cenozoic tectonics of the northern edge of the Tibetan plateau: fission-track constraints. Tectonophysics 343, 111–134.
- Jolivet, M., Brunel, M., Seward, D., Xu, Z., Yang, J., Malavieille, J., Roger, F., Leyreloup, A., Arnaud, N., Wu, C., 2003. Neogene extension and volcanism in the Kunlun fault zone, northern Tibet: new constraints on the age of the Kunlun Fault. Tectonics 22 (5), 1052.
- Ke, X., Ji, J.L., Zhang, K.X., Kou, X.H., Song, B.W., Wang, C.W., 2013.
 Magnetostratigraphy and anisotropy of magnetic susceptibility of the Lulehe
 Formation in the northeastern Qaidam Basin. Acta Geol. Sin. Engl. Ed. 87, 576–587.
- Li, J., Fang, X., Song, C., Pan, B., Ma, Y., Yan, M., 2014. Late Miocene-quaternary rapid stepwise uplift of the Tibetan Plateau and its effects on climatic and environmental changes. Quat. Res. 81 (3), 400–423.
- Li, B.S., Yan, M.D., Zhang, W.L., Fang, X.M., Meng, Q.Q., Zan, J.B., Chen, Y., Zhang, D. W., Yang, Y.P., Guan, C., 2017. New paleomagnetic constraints on middle Miocene strike-slip faulting along the middle Altyn Tagh Fault. J. Geophys. Res. Solid Earth 122, 4106–4122.
- Liu, Z.H., Yang, J.G., Wang, C.B., Liu, Z.W., Zhang, L.G., 2004. Nature of Mesozoic basins in the northern edge of Qaidam Basin. Oil Gas Geol. 25 (4), 620–624 (In Chinese with English abstract).
- Liu, S., Zhang, G., Pan, F., Zhang, H., Wang, P., Wang, K., Wang, Y., 2013. Timing of Xunhua and Guide basin development and growth of the northeastern Tibetan Plateau, China. Basin Res. 25 (1), 74–96.
- Liu, R., Allen, M., Zhang, Q., Du, W., Cheng, X., Holdsworth, R., Guo, Z., 2017. Basement controls on deformation during oblique convergence: transpressive structures in the western Qaidam Basin, northern Tibetan Plateau. Lithosphere 9, 583–594.
- Liu, R.C., Chen, Y., Yu, X.J., Du, W., Cheng, X., Guo, Z.J., 2019. An analysis of distributed strike-slip shear deformation of the Qaidam Basin, Northern Tibetan Plateau. Geophys. Res. Lett. 46, 4202–4211.
- Lou, Q.Q., Xiao, A.C., Yang, H., Huang, H.S., Ding, W.X., Shen, Z.Y., Wang, L., Chen, Y.Z., Shen, Y., Wang, L.Q., Zhou, S.P., 2009. Characteristics of Mesozoic basin of the northern Qaidam: a case study on Dachaidan depression. Geol. J. China Univ. 15 (3), 407–416 (In Chinese with English abstract).
- Lu, H.J., Xiong, S.F., 2009. Magnetostratigraphy of the Dahonggou section, northern Qaidam Basin and its bearing on Cenozoic tectonic evolution of the Qilian Shan and Altyn Tagh Fault. Earth Planet. Sci. Lett. 288, 539–550.

- Luo, Q., 2008. Discussion on genetic type of the Qaidam Basin. Pet. Geol. Exp. 30 (2), 115–120 (In Chinese with English abstract).
- Mao, L.G., Xiao, A.C., Zhang, H.W., Wu, Z.K., Wang, L.Q., Shen, Y., Wu, L., 2016. Structural deformation pattern within the NW Qaidam Basin in the Cenozoic era and its tectonic implications. Tectonophysics 687, 78–93.
- Meng, Q.R., Hu, J.M., Yang, F.Z., 2001. Timing and magnitude of displacement on the Altyn Tagh fault: constraints from stratigraphic correlation of adjoining Tarim and Qaidam basins, NW China. Terra Nova 13 (2), 86–91.
- Métivier, F., Gaudemer, Y., Tapponnier, P., Meyer, B., 1998. Northeastward growth of the Tibet plateau deduced from balanced reconstruction of two depositional areas: the Qaidam and Hexi Corridor basins, China. Tectonics 17 (6), 823–842.
- Meyer, B., Tapponnier, P., Bourjot, L., Metivier, F., Gaudemer, Y., Peltzer, G., Guo, S.M., Chen, Z.T., 1998. Crustal thickening in Gansu-Qinghai, lithospheric mantle subduction, and oblique, strike-slip controlled growth of the Tibet plateau. Geophys. J. Int. 135 (1). 1-47.
- Molnar, P., 2005. Mio-Pliocene growth of the Tibetan Plateau and evolution of East Asian climate. Palaeontol. Electron. 8, 1–23.
- Molnar, P., Stock, J.M., 2009. Slowing of India's convergence with Eurasia since 20 Ma and its implications for Tibetan mantle dynamics. Tectonics 28, TC3001.
- Molnar, P., Tapponnier, P., 1975. Cenozoic tectonics of Asia: effects of a continental collision. Science 189, 419–426.
- Najman, Y., Appel, E., Boudagher-Fadel, M., Bown, P., Carter, A., Garzanti, E., Godin, L., Han, J.T., Liebke, U., Oliver, G., Parrish, R., Vezzoli, G., 2010. Timing of India-Asia collision: geological, biostratigraphic, and palaeomagnetic constraints. J. Geophys. Res. Solid Earth 115, B12416.
- Peltzer, G., Tapponnier, P., 1988. Formation and evolution of strike slip faults, rifts, and basins during the India-Asia collision: an experimental approach. J. Geophys. Res. 93, 15,085–15,117.
- Ritts, B.D., Biffi, U., 2000. Magnitude of post-Middle Jurassic (Bajocian) displacement on the central Altyn Tagh fault system, Northwest China. Geol. Soc. Am. Bull. 112 (1), 61–74.
- Ritts, B.D., Yue, Y., Graham, S.A., 2004. Oligocene-Miocene tectonics and sedimentation along the Altyn Tagh Fault, Northern Tibetan Plateau: analysis of the Xorkol, Subei, and Aksay Basins. J. Geol. 112 (2), 207–229.
- Rowley, D.B., 1996. Age of initiation of collision between India and Asia: a review of stratigraphic data. Earth Planet. Sci. Lett. 145 (1–4), 1–13.
- Royden, L.H., Burchfiel, B.C., King, R.W., Wang, E., Chen, Z., Shen, F., Liu, Y., 1997.
 Surface deformation and lower crustal flow in eastern Tibet. Science 276 (5313), 788–790.
- Rumelhart, P., Yin, A., Cowgill, E., Butler, R., Zhang, Q., Feng, W.X., 1999. Cenozoic vertical-axis rotation of the Altyn Tagh fault system. Geology 27 (9), 819–822.
- Searle, M., Elliott, J., Phillips, R., Chung, S.L., 2011. Crustal-lithospheric structure and continental extrusion of Tibet. Geophys. J. Int. 168, 633–672.
- Sobel, E.R., Arnaud, N., Jolivet, M., Ritts, B.D., Brunel, M., 2001. Jurassic to Cenozoic exhumation history of the Altyn Tagh range, Northwest China, constrained by 40 Ar/ 39 Ar and apatite fission track thermochronology. Geol. Soc. Am. Memo. 194, 247–267.
- Song, C.H., 2006. Tectonic Uplift and Cenozoic Sedimentary Evolution in the Northern Margin of the Tibetan Plateau. Ph.D. thesis. Lanzhou University, Lanzhou (in Chinese).
- Sun, Z.M., Yang, Z.Y., Pei, J.L., Ge, X.H., Wang, X.S., Yang, T.S., Li, W.M., Yuan, S.H., 2005. Magnetostratigraphy of Paleogene sediments from northern Qaidam Basin, China: implications for tectonic uplift and block rotation in northern Tibetan plateau. Earth Planet. Sci. Lett. 237, 635–646.
- Sun, Z.C., Jing, M.C., Sun, N.D., Lu, Y.L., Cao, L., 2007. Discussion on boundary between the upper and lower members of Xiaganchaigou Formation of Paleogene in Well Kun-2, Qaidam Basin. J. Palaeogeogr. 9 (6), 611–618 (in Chinese).
- Sylvester, A.G., 1988. Strike-slip faults. Geol. Soc. Am. Bull. 100, 1666-1703.
- Tapponnier, P., Peltzer, G., Armijo, R., 1986. On the mechanics of the collision between India and Asia. Geol. Soc. Lond., Spec. Publ. 19 (1), 113–157.
- Tapponnier, P., Meyer, B., Avouac, J.P., Peltzer, G., Gaudemer, Y., Guo, S.M., Xiang, H. F., Yin, K.L., Chen, Z.T., Cai, S.H., Dai, H.G., 1990. Active thrusting and folding in the Qilian Shan, and decoupling between upper crust and mantle in northeastern Tibet. Earth Planet. Sci. Lett. 97, 382–403.
- Tapponnier, P., Xu, Z.Q., Roger, F., Meyer, B., Arnaud, N., Wittlinger, G., Yang, J.S., 2001. Oblique stepwise rise and growth of the Tibet Plateau. Science 294 (5547), 1671–1677.
- Tikoff, B., Peterson, K., 1998. Physical experiments of transpressional folding. J. Struct. Geol. 20, 661–672.
- Titus, S.J., Housen, B., Tikoff, B., 2007. A kinematic model for the Rinconada fault system in central California based on structural analysis of en echelon folds and paleomagnetism. J. Struct. Geol. 29, 961–982.
- Van Hinsbergen, D.J., Lippert, P.C., Dupont-Nivet, G., McQuarrie, N., Doubrovine, P.V., Spakman, W., Torsvik, T.H., 2012. Greater India Basin hypothesis and a two-stage Cenozoic collision between India and Asia. Proc. Natl. Acad. Sci. U. S. A. 109, 7659–7664.
- Wan, J.L., Wang, Y., Li, Q., Wang, F., Wang, E., 2001. FT evidence of northern Altyn uplift in late-Cenozoic. Bull. Mineral. Petrol. Geochem. 20 (4), 222–224 (In Chinese with English abstract).
- Wang, E., 1997. Displacement and timing along the northern strand of the Altyn Tagh fault zone, northern Tibet. Earth Planet. Sci. Lett. 150 (1–2), 55–64.
- Wang, Y., Zhang, X., Wang, E., Zhang, J., Li, Q., Sun, G., 2005. ⁴⁰Ar/³⁹Ar thermochronological evidence for formation and Mesozoic evolution of the northern-central segment of the Altyn Tagh fault system in the northern Tibetan Plateau. Geol. Soc. Am. Bull. 117 (9), 1336–1346.

Wang, E., Xu, F.Y., Zhou, J.X., Wan, J.L., Burchfiel, B.C., 2006. Eastward migration of the Qaidam basin and its implications for Cenozoic evolution of the Altyn Tagh fault and associated river systems. Geol. Soc. Am. Bull. 118, 349–365.

- Wang, L., Xiao, A.C., Gong, Q.L., Liu, D., Wu, L., Zhou, S.P., Shen, Z.Y., Lou, Q.Q., Sun, X. W., 2010. The unconformity in Miocene sequence of the western Qaidam Basin and its tectonic significance. Sci. China Earth Sci. 53, 1126–1133.
- Wang, S.L., Wu, W.J., Li, Q.H., Li, C., Li, Y.X., Chen, Y., Wang, L.S., Xu, M.J., Guo, Z., 2020. Coseismic underground rupture, geometry, historical surface deformations, and seismic potentials of the 28 March 2019 Mw 5.04 Mangya earthquake fault. Tectonics 39. https://doi.org/10.1029/2020TC006244 e2020TC006244.
- Wittlinger, G., Tapponnier, P., Poupinet, G., Mei, J., Danian, S., Herquel, G., Masson, F., 1998. Tomographic evidence for localized lithospheric shear along the Altyn Tagh Fault. Science 282, 74–76.
- Woodcock, N.H., Fischer, M., 1986. Strike-slip duplexes. J. Struct. Geol. 8, 725–735.
- Wu, L., Xiao, A.C., Wang, L.Q., Shen, Z.Y., Zhou, S.P., Chen, Y.Z., Wang, L., Liu, D., Guan, J.Y., 2011. Late Jurassic-Early Cretaceous northern Qaidam Basin, NW China: implications for the earliest Cretaceous intracontinental tectonism. Cretac. Res. 32 (4), 552–564.
- Wu, L., Xiao, A.C., Yang, S.F., Wang, L.Q., Mao, L.G., Wang, L., Dong, Y.P., Xu, B., 2012. Two-stage evolution of the Altyn Tagh Fault during the Cenozoic: new insight from provenance analysis of a geological section in NW Qaidam Basin, NW China. Terra Nova 24 (5), 387–395.
- Wu, L., Lin, X.B., Cowgill, E., Xiao, A.C., Cheng, X.G., Chen, H.L., Zhao, H.F., Shen, Y., Yang, S.F., 2019. Middle Miocene reorganization of the Altyn Tagh fault system, northern Tibetan Plateau. Geol. Soc. Am. Bull. 131 (7–8), 1157–1178.
- Wu, W.J., Yuan, J.Y., Wang, J.G., Shi, Y.J., Chen, Y., Zou, K.Z., Jia, D., 2020. A Late Neogene framework and transpressional system within the Yingxiongling Range, western Qaidam Basin, Northeast Tibetan Plateau: insights from seismic reflection profiles and active tectonics. J. Asian Earth Sci. 198, 104061.
- Xiao, W., Windley, B.F., Yong, Y., Yan, Z., Yuan, C., Liu, C., Li, J., 2009. Early Paleozoic to Devonian multiple-accretionary model for the Qilian Shan, NW China. J. Asian Earth Sci. 35 (3-4), 323–333.
- Yang, F., Ma, Z.Q., Xu, T.C., Ye, S.J., 1992. A Tertiary paleomagnetic stratigraphic profile in Qaidam Basin. Acta Pet. Sin. 13, 97–101.
- Yang, Y.T., Ritts, B., Zou, C.N., Xu, T.G., Zhang, B.M., Xi, P., 2003. Upper Triassic-Middle Jurassic stratigraphy and sedimentology in the NE Qaidam Basin, NW China: petroleum geological significance of new outcrop and subsurface data. J. Pet. Geol. 26 (4), 429–449.
- Yang, Y.T., Zhang, B.M., Zhao, C.Y., Xu, T.G., 2004. Mesozoic source rocks and petroleum systems of the northeastern Qaidam Basin, northwest China. AAPG Bull. 88 (1), 115–125.
- Ye, D., Zhong, X., Yao, Y.F., Yang, F., Zhang, S., Jiang, Z., Wang, Y., 1993. Tertiary Strata in Chinese Petroliferous Provinces (Volume I)-the General. Petroleum Industry Press, Beijing, pp. 156–159 (in Chinese).
- Yin, A., Harrison, T.M., 2000. Geologic evolution of the Himalayan-Tibetan Orogen. Annu. Rev. Earth Planet. Sci. 28 (1), 211–280.
- Yin, A., Rumelhart, P.E., Butler, R., Cowgill, E., Harrison, T.M., Foster, D.A., Ingersoll, R. V., Qing, Z., Zhou, X.Q., Wang, X.F., Hanson, A., Raza, A., 2002. Tectonic history of the Altyn Tagh fault system in northern Tibet inferred from Cenozoic sedimentation. Geol. Soc. Am. Bull. 114, 1257–1295.
- Yin, A., Dang, Y.Q., Zhang, M., McRivette, M.W., Burgess, W.P., Chen, X.H., 2007. Cenozoic tectonic evolution of Qaidam basin and its surrounding regions (part 2): wedge tectonics in southern Qaidam basin and the Eastern Kunlun Range. Geol. Soc. Am. Spec. Pap. 433, 369–390.
- Yin, A., Dang, Y.Q., Wang, L.C., Jiang, W.M., Zhou, S.P., Chen, X.H., Gehrels, G.E., McRivette, M.W., 2008a. Cenozoic tectonic evolution of Qaidam basin and its surrounding regions (part 1): the southern Qilian Shan-Nan Shan thrust belt and northern Qaidam basin. Geol. Soc. Am. Bull. 120, 813–846.
- Yin, A., Dang, Y.Q., Zhang, M., Chen, X.H., McRivette, M.W., 2008b. Cenozoic tectonic evolution of the Qaidam basin and its surrounding regions (part 3): structural geology, sedimentation, and regional tectonic reconstruction. Geol. Soc. Am. Bull. 120. 847–876.
- Yin, J.G., Zhang, S.Y., Lu, X.C., Wu, Z.X., Guo, H., Ju, Y.W., 2019. Controls of the Altyn Tagh Fault on the Early-Middle Miocene sedimentation in the Honggouzi Area, Qaidam Basin, Western China. J. Asian Earth Sci. 181, 103908.
- Yu, F., Wang, Y., Li, X., Feng, Z., 2011. Deformation characteristics and genesis simulation of the Shizigou-Youshashan structural belt in Qaidam Basin. Geotecton. Metallog. 2, 6.
- Yu, X., Huang, B., Guan, S., Fu, S., Cheng, F., Cheng, X., Zhang, T., Guo, Z., 2014a. Anisotropy of magnetic susceptibility of Eocene and Miocene sediments in the Qaidam Basin, Northwest China: implication for Cenozoic tectonic transition and depocenter migration. Geochem. Geophys. Geosyst. 15 (6), 2095–2108.
- Yu, X.J., Fu, S.T., Guan, S.W., Huang, B.C., Cheng, F., Cheng, X., Zhang, T., Guo, Z.J., 2014b. Paleomagnetism of Eocene and Miocene sediments from the Qaidam basin: implication for no integral rotation since the Eocene and a rigid Qaidam block. Geochem. Geophys. Geosyst. 15 (6), 2109–2127.
- Yu, X.J., Guo, Z.J., Zhang, Q.Q., Cheng, X., Du, W., Wang, Z.D., Bian, Q., 2017. Denan depression controlled by northeast-directed Olongbulak Thrust Zone in northeastern Qaidam basin: implications for growth of northern Tibetan Plateau. Tectonophysics 717, 116–126.
- Yuan, D.Y., Ge, W.P., Chen, Z.W., Li, C.Y., Wang, Z.C., Zhang, H.P., Zhang, P.Z., Zheng, D.W., Zheng, W.J., Craddock, W.H., 2013. The growth of northeastern Tibet and its relevance to large-scale continental geodynamics: a review of recent studies. Tectonics 32, 1358–1370.
- Yue, Y.J., Liou, J.G., 1999. Two-stage evolution model for the Altyn Tagh Fault, China. Geology 27, 227–230.

- Yue, Y.J., Ritts, B.D., Graham, S.A., 2001. Initiation and long-term slip history of the Altyn Tagh Fault. Int. Geol. Rev. 43 (12), 1087–1093.
- Yue, Y.J., Ritts, B.D., Graham, S.A., Wooden, J.L., Gehrels, G.E., Zhang, Z., 2004a. Slowing extrusion tectonics: Lowered estimate of post-Early Miocene slip rate for the Altyn Tagh fault. Earth Planet. Sci. Lett. 217, 111–122.
- Yue, Y.J., Ritts, B.D., Hanson, A.D., Graham, S.A., 2004b. Sedimentary evidence against large strike-slip translation on the Northern Altyn Tagh fault, NW China. Earth Planet. Sci. Lett. 228, 311–323.
- Yue, Y.J., Graham, S.A., Ritts, B.D., Wooden, J.L., 2005. Detrital zircon provenance evidence for large-scale extrusion along the Altyn Tagh fault. Tectonophysics 406 (3–4), 165–178.
- Yun, L., Zhang, J., Wang, J., Yang, X.P., Qu, J.F., Zhang, B.H., Zhang, H., 2020. Active deformation to the north of the Altyn Tagh Fault: constraints on the northward growth of the northern Tibetan Plateau. J. Asian Earth Sci. https://doi.org/10.1016/ i.iseaes.2020.104312.
- Zhang, W.L., 2006. The High Precise Cenozoic Magnetostratigraphy of the Qaidam Basin and Uplift of the Northern Tibetan Plateau. Ph.D. thesis. Lanzhou University, Lanzhou (in Chinese).
- Zhang, W.L., Appel, E., Fang, X.M., Song, C.H., Cirpka, O., 2012. Magnetostratigraphy of deep drilling core SG-1 in the western Qaidam Basin (NE Tibetan Plateau) and its tectonic implications. Quat. Res. 78, 139–148.
- Zhang, W.L., Appel, E., Fang, X.M., Song, C.H., Setzer, F., Herb, C., Yan, M.D., 2014.
 Magnetostratigraphy of drill-core SG-1b in the western Qaidam Basin (NE Tibetan Plateau) and tectonic implications. Geophys. J. Int. 197, 90–118.

- Zhang, T., Fang, X.M., Wang, Y.D., Song, C.H., Zhang, W.L., Yan, M.D., Han, W.X., Zhang, D.W., 2018. Late Cenozoic tectonic activity of the Altyn Tagh range: constraints from sedimentary records from the Western Qaidam Basin, NE Tibetan Plateau. Tectonophysics 737, 40–56.
- Zhang, W.L., Appel, E., Fang, X.M., Setzer, F., Song, C.H., Meng, Q.Q., Yan, M.D., 2020.
 New paleomagnetic constraints on syntectonic growth strata in the western Qaidam Basin, NE Tibetan Plateau. Tectonophysics 780, 228401.
- Zhao, J.F., Zeng, X., Tian, J.X., Hu, C., Wang, D., Yan, Z.D., Wang, K., Zhao, X.D., 2020. Provenance and paleogeography of the Jurassic Northwestern Qaidam Basin (NW China): evidence from sedimentary records and detrital zircon geochronology. J. Asian Earth Sci. 190, 104060.
- Zheng, D., Clark, M.K., Zhang, P., Zheng, W., Farley, K.A., 2010. Erosion, fault initiation and topographic growth of the North Qilian Shan (northern Tibetan Plateau). Geosphere 6 (6), 937–941.
- Zhou, J., Xu, F., Wang, T., Cao, A., Yin, C., 2006. Cenozoic deformation history of the Qaidam Basin, NW China: results from cross-section restoration and implications for Qinghai-Tibet Plateau tectonics. Earth Planet. Sci. Lett. 243, 195–210.
- Zhuang, G., Hourigan, J.K., Ritts, B.D., Kent-Corson, M.L., 2011. Cenozoic multiplephase tectonic evolution of the northern Tibetan Plateau: constraints from sedimentary records from Qaidam basin, Hexi Corridor, and Subei Basin, northwest China. Am. J. Sci. 311 (2), 116–152.